ISSN 0965-545X, Polymer Science, Series A, 2023, Vol. 65, No. 4, pp. 312–336. © Pleiades Publishing, Ltd., 2023.
ISSN 0965-545X, Polymer Science, Series A, 2023. © Pleiades Publishing, Ltd., 2023.
Russian Text © The Author(s), 2023, published in Vysokomolekulyarnye Soedineniya, Seriya A, 2023, Vol. 65, No. 4, pp. 249–274.

POLYELECTROLYTES

Polymer Electrolytes Based on Polybenzimidazole, Poly(Vinylidene Fluoride-*co*-Hexafluoropropylene), and Ionic Liquids

L. P. Safonova[a] and L. E. Shmukler[a,*]

[a] *Krestov Institute of Solutions Chemistry, Russian Academy of Sciences, Ivanovo, 153045 Russia*

**e-mail: les@isc-ras.ru*

Received February 7, 2023; revised April 17, 2023; accepted July 3, 2023

Abstract—Ionic liquids, salts with melting temperature below 100°C, have continuously attracted research interest. Introduction of ionic liquids in a polymer matrix affords polymer electrolytes exhibiting extremely high electroconductivity and electrochemical stability, membranes on their basis possessing good mechanical properties. Diversity of the polymers/copolymers suitable as the matrix as well as practically unlimited variety of ionic liquids (obtained via variation of the anion-cation composition and additional modification of the ions chemical structure) have afforded the polymer electrolytes with a wide range of the physico-chemical properties. In this study, the attention has been primarily focused on the results published over the recent decades and related to investigation of electrolytes for electrochemical devices, in which the membranes based on polybenzimidazole (meta-PBI), the poly(vinylidene fluoride-*co*-hexafluoropropylene) (PVdF-HFP) copolymer, and ammonium or imidazolium ionic liquids have been used. Various types of polymer electrolytes differing in the composition and the application range have been considered in this study: polymer + ionic liquid, polymer + ionic liquid + acid, and polymer + ionic liquid + lithium/sodium salt. Moreover, the influence of the fillers, introduced in the above-said polymer electrolytes to improve the properties and resolve the issue of the ionic liquid retention in the membrane, has been discussed. This report presents vast data sets (tables) on the electroconductivity and thermal stability of more than 100 polymer electrolytes, which are demanded by the broad journal audience.

DOI: 10.1134/S0965545X23701080

INTRODUCTION

Ionic liquids, salts with melting temperature below 100°C, have continuously attracted research interest. Owing to their unique properties, such as low vapor pressure, high thermal and electrochemical stability, low flammability, and high ionic conductivity, they have been applied in various fields: in organic synthesis, as materials for electrochemical energy storage and conversion devices, for separation and isolation of substances, as catalysts and heat transfer agents [1–6]. Many reviews, original reports, and patents on the preparation, properties, and application of ionic liquids have been recently published [7–16]. Ionic liquids have been used to synthesize novel materials [5, 17–21] and studied as potential solvents for extraction and separation of substances [22–26] or as electrolytes for different electrochemical devices [27–34]. Ionic liquids have been widely applied in biotechnology and pharmaceutics [35–38]. Many ionic liquids have been synthesized and characterized; their properties, structure, and applications have been reviewed in [16, 39–48].

Ionic liquids used in various electronic devices can act as electrolytes in the pure form as well as components of polymer electrolyte. Two major classes of polymer electrolytes based on ionic liquids are as follows: polymer + ionic liquid and polymerized ionic liquid. Polymerized ionic liquids can be prepared either via polymerization of a monomeric ionic liquid or via modification of a polymer. Herein, polymer electrolytes of the polymer + ionic liquid type as well as composite systems on their basis will be considered. In such systems charge transfer occurs mainly in the liquid phase, whereas the polymer matrix retains the liquid electrolyte in the pores. Mechanism of the ion transport in such polymer electrolytes (the liquid-like mechanism) has been considered in [49]; it has been shown that their ionic conductivity correlates with the segmental relaxation of the polymer matrix, in contrast to the superionic glasses and crystals, in which the ions diffusion occurs in a practically frozen structure via the solid-like mechanism. Since ionic liquid introduced in the polymer matrix acts as plasticizer, such polymer electrolytes are also known as gel electrolytes. Furthermore, the introduction of ionic liquid in the polymer matrix allows polymer electrolytes with

high electroconductivity and electrochemical stability, and the membranes on their basis exhibit flexibility and good mechanical properties. Diversity of the polymers/copolymers suitable as the matrix and practically unlimited number of ionic liquids obtained via variation of the anion-cation composition or additional modification of the ions chemical structure afford polymer electrolytes with a broad range of physico-chemical properties. According to the Scopus database, nearly 100% of the publications on polymer electrolytes based on ionic liquids (the "Ionic Liquid Polymer Electrolytes" query) are related to their application in batteries, supercapacitors, and fuel and solar cells. In the case of supercapacitors, the nature of the ions providing charge transport is not important, but it is essential to ensure proton conductivity as far as fuel cells are concerned. Hence, aprotic ionic liquids are mainly used in supercapacitors, whereas protic ones are considered for fuel cells applications. In the proton-conductive membranes of the polymer + ionic liquid + acid type, the ionic liquid can act as plasticizer as well as be involved in the proton transfer.

Owing to their properties, ionic liquids provide a good alternative to organic solvents used in polymer electrolytes for lithium batteries (polymer + ionic liquid + lithium/sodium salt), since efficiency of organic solvents is limited by their volatility, high flammability, and mechanical instability at high temperature. Moreover, growth of lithium dendrites is among the factors limiting the life cycle of lithium metal batteries. It has been shown that polymer electrolytes based on ionic liquids can suppress the dendrites growth [50–52].

Mechanical, thermal, and chemical properties of polymer electrolytes can be improved via the introduction of fillers, for example, silicon dioxide, titanium dioxide, zirconium dioxide, graphene oxide, carbon nanotubes, and layered silicates [53–59]. The filler can be either covalently linked to the polymer matrix or the ionic liquid, or remain not bound. Plasticizers (for instance, organic solvents such as PC, EC, and DMC) can be introduced in polymer electrolytes to increase their electroconductivity.

A series of reviews on polymer electrolytes based on ionic liquids (polymer–ionic liquid) have been recently published [60–64]. For example, historical overview of the methods of preparation and investigation of such polymer electrolytes has been given in [64], along with description of their modification methods and application range. It has been marked that high price and relatively low mechanical strength remain the key obstacles limiting wide application of polymer electrolytes based on ionic liquids.

The use of natural macromolecules to reduce the price, creation of composite polymer systems to improve the mechanical strength, preparation of polymerized ionic liquids with enhanced electrochemical properties, and introduction of nanomaterials to improve the interface contact and the ionic transport have been considered among major directions of the research in the field of development of reliable and highly efficient polymer electrolytes of the polymer–ionic liquid type. The role of various additives (plasticizers and fillers) in the targeted development of polymer electrolytes has been discussed in [65, 66].

Recent progress in the development of innovative polymer electrolytes based on ionic liquid (polymer–ionic liquid) for energy harvesting and storage applications has been discussed in [61]. Special attention has been paid to the effect of the ionic liquid on thermal stability, melting and vitrification temperatures, and degree of crystallinity of the polymer matrix as well as on the polymer electrolytes electroconductivity. It has been stated that increase in the content of ionic liquid in the polymer enhances the ionic conductivity, due to the increase in the number of free charge carriers as well as plasticizing effect of the ionic liquid on the crystalline regions of the polymer matrix. The plasticizing effect of the ionic liquid also leads to the decrease in the melting and vitrification temperatures, reduction in the degree of crystallinity, and deterioration of the mechanical stability of the polymer electrolyte. Polymer membranes based on ionic liquid are thermally stable over broad temperature range of ~200–400°C. In general, the review [61] has concluded that polymer electrolytes based on ionic liquids are advantageous over polymer electrolytes obtained via immobilization of liquid electrolytes (solution of a salt in aprotic polar organic solvents such as EC, PC, DMF, etc.) in polymer matrix.

The reports on proton-exchange membranes based on protic ionic liquids immobilized in a polymer for the application in fuel cells have been reviewed in [67–72]. The authors have analyzed the issues related to the development of this promising class of the membranes and recommended future research directions. Major attention in reviews [67, 68, 70] has been paid to electrolyte membranes produced of ionic liquids in combination with polybenzimidazole. It has been shown that electroconductivity of the polymer electrolyte membranes can be increased via the introduction of fillers (such as carbon-based materials, inorganic fillers, and metal-organic frameworks) as well as modification of the structure of polybenzimidazole [68]. The role of protic ionic liquids introduced in polymer membranes of different types: Nafion, sulfonated poly(ether ether ketone), poly(vinyl alcohol), polybenzimidazole, sulfonated polyimide, and poly(vinylidene fluoride-*co*-hexafluoropropylene) has been discussed in [69, 71]. Since the perfluorosulfonic acid polymers (Nafion) are the most widespread and commercially available polymer electrolyte membrane materials, properties of novel membrane materials are often compared to Nafion [73–78]. However, the properties of Nafion membranes are deteriorated at temperature above 100°C, due to the membrane

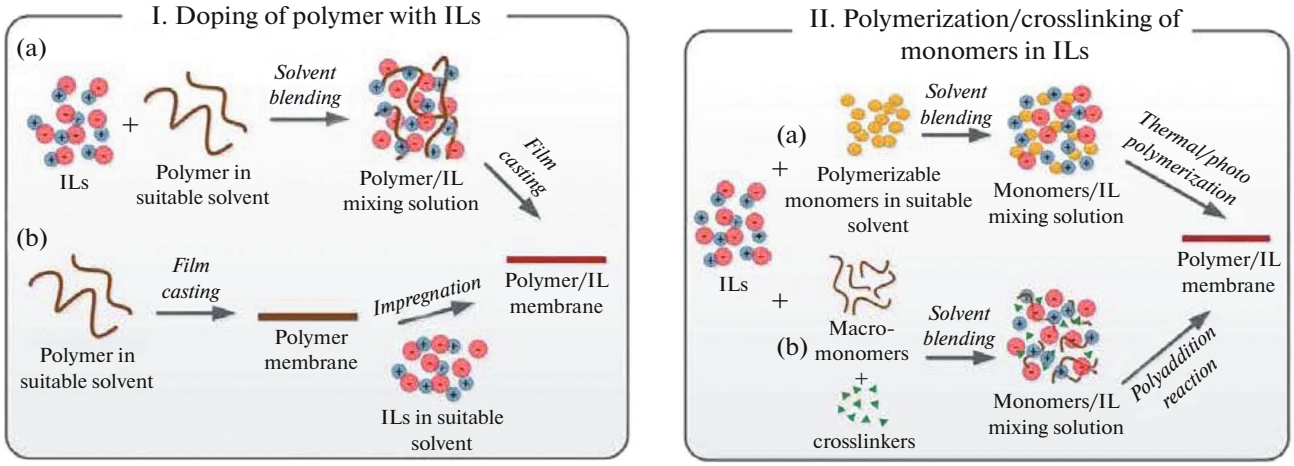

Fig. 1. Scheme of production of polymer electrolytes based on ionic liquid. Reproduced with permission from [84]. Color illustrations are available in the online version.

degradation resulting decreased conductivity. Taking advantage of ionic liquids allows production of polymer electrolytes operating at temperature above 100°C under anhydrous conditions. Furthermore, the ways to resolve the issues related to the use of protic ionic liquids in polymer membranes, which are due to their leaching and poor mechanical stability at elevated temperature have been considered in [69]; the potential of hybrid (composite) polymer–ionic liquid–inorganic filler membranes for the application in high-temperature fuel cells has been shown.

Electrochemical and physico-chemical properties of the ionic liquids as well as the derived polymer electrolytes, essential for the application in lithium-ion batteries and supercapacitors, have been considered in [28, 79–82]. Recent progress in the field of ionic liquid-based electrolytes for lithium-ion batteries has been generalized in [81]. It has been shown that physico-chemical properties of such electrolytes are usually determined by the chemical composition and the cation–anion interactions, whereas their thermal stability (temperature of the decomposition onset above 200°C) ensures excellent electrochemical parameters of lithium-ion batteries at elevated temperature. Moreover, it has been shown that many polymer electrolytes exhibit wider electrochemical window than commercial organic-based electrolytes, which allows the use of the former ones as high-voltage cathode materials. Furthermore, rational design of hybrid electrolytes based on ionic liquids, including ionic liquid–organic solvent hybrid electrolyte, mixed cation/anion electrolyte, and ionic liquid–water hybrid electrolyte, can significantly improve the electrochemical properties, which opens wide prospects for modification of lithium-ion batteries.

Review [83] has provided comparative analysis of properties of hybrid electrolytes for supercapacitors, composition of which is determined by a combination of the following components: water, organic solvent, ionic liquid, and polymer. For the novel hybrid electrolytes, synergetic effect of the components mixing has been marked, leading to improved electrochemical parameters of the supercapacitors (broadened operational voltage window, increased ionic conductivity, and enhanced stability).

Procedures for Preparation and Investigation of Polymer Electrolytes Based on Ionic Liquids

The methods to prepare polymer electrolytes consisting of polymer matrix and ionic liquid can be divided into two groups: doping of the polymer with ionic liquid (Fig. 1, I) and polymerization or crosslinking of monomers in the ionic liquid (Fig. 1, II).

Doping of polymers with ionic liquids is possible either via impregnation of the polymer with the ionic liquid (the swelling method) or via dissolution of the polymer and ionic liquid in an organic solvent, followed by casting the solution and drying on a support (the casting method). The casting method allows control over concentration of ionic liquid in the polymer electrolyte as well as production of composite materials via introduction of inorganic fillers in the solution. It should be noted that the use of organic solvent makes this approach environmentally unfriendly. Impregnation of the prepared polymer matrix with a ionic liquid is a facile method to obtain polymer electrolytes. However, the composition range of the prepared polymer electrolytes is limited by the swelling degree of the polymer in the ionic liquid; at the same time, this method affords control over the polymer matrix morphology.

Owing to good solubility of most of common monomers in ionic liquids, polymerization/crosslinking directly in the ionic liquid yields polymer electro-

lytes with high ionic conductivity. As far as this approach is considered, compatibility between the polymer and the ionic liquid is an important factor.

Since the polymer electrolytes are majorly used in electrochemical devices, their important parameters include electroconductivity, electrochemical window, and ion transport number (also known as transference number). The electrochemical window is determined by means of voltammetry with linear scanning, whereas electroconductivity is assessed by means of impedance spectroscopy. The transference number can be measured using the Maxwell–Wagner polarization method, the direct current polarization test, or the combined Bruce–Vincent method.

Besides the mentioned important electrochemical properties, polymer electrolytes should also exhibit high thermal stability (analyzed by means of thermogravimetry) and mechanical strength. Moreover, the differential scanning calorimetry method allows determination of temperature of the phase transitions occurring in the polymer electrolyte on heating. To assess the stability of the membranes in the oxidizing media (important for the fuel cells applications), the test with the Fenton's reagent is used.

In the studies of polymer electrolytes, special attention is paid to elucidation of the relationship between their properties and the structure as well as character of the interactions of the ionic liquid with the polymer functional groups. For example, X-ray diffraction method can be used to investigate the crystalline and amorphous regions in the polymer, scanning and transmission electron microscopy allows assessment of the surface and cross-section morphology of the membranes, whereas spectral methods (IR, Raman, NMR) probe the possible interactions between the polymer electrolyte components.

In this review, we mainly focused on the reports published over the recent decade, related to the research on the electrolytes for electrochemical devices produced of the membranes based on polybenzimidazole (**PBI**) and poly(vinylidene fluoride-*co*-hexafluoropropylene) (**PVdF-HFP**) with alkylammonium and alkylimidazolium ionic liquids, the best studied among other ionic liquids. The wide use of PVdF–HFP and PBI as matrices of electrolyte membranes is due to their high chemical, thermal, and mechanical stability. Over 30% of the publications in the above-mentioned Scopus query have considered the membranes based on these polymers. The choice of the alkylammonium and alkylimidazolium ionic liquids is due to the fact that their properties are the best studied among other ionic liquids.

Herein, we considered various types of polymer electrolytes based on the ionic liquids, differing in the composition and the application range: polymer + ionic liquid, polymer + ionic liquid + acid, polymer + ionic liquid + lithium/sodium salt; furthermore, we considered the effect of different fillers on the properties of the above-listed polymer electrolytes.

Polymer Electrolytes Based on Polybenzimidazole

Polymer electrolytes with polybenzimidazoles ([poly(2,2'-(1,3-phenylene)-5,5'-di(benzimidazole)] ***meta*-PBI**, [poly(2,2'-(1,4-phenylene)-5,5'-di(benzimidazole)] *para*-PBI, [poly(2,5-benzimidazole)] **AB-PBI**, pyridine-based PBI, [poly-(2,2'-(2,5-dihydroxy-1,4-phenylene)-5,5'-dibenzimidazole)] 2OH-PBI, and others) as the polymer matrix are mainly applied in fuel cells.

The best studied polybenzimidazoles are *meta*-PBI and AB-PBI, the former one being considered in this review.

Poly-2,2'-(*m*-phenylene)-5,5'-di(benzimidazole) is an aromatic heterocyclic polymer:

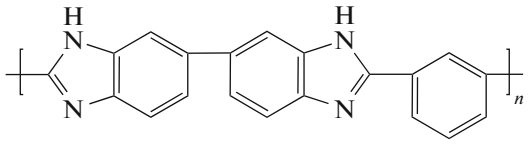

Polybenzimidazole exhibits rigid rodlike molecular structure with numerous H-bonds between the molecular chains with the π–π-packing, which hinders its dissolution in many organic solvents. Its special features are high chemical and thermal (up to 310°C) stability, excellent mechanical properties, good moisture yielding capacity, and good thermooxidative stability (above 80°C). Table 1 lists composition and selected properties of polymer electrolytes based on polybenzimidazole and ionic liquids.

Recent progress in the field of application of composite polybenzimidazole-based membranes in high-temperature fuel cells has been generalized in [68–71, 104–106].

(Polybenzimidazole–Ionic Liquid)–Acid Polymer Electrolyte

Pure polybenzimidazole exhibits low proton conductivity (10^{-9} mS/cm), therefore it should be doped with an acid to achieve high electroconductivity. In the acid-doped polybenzimidazole, proton transfer mainly occurs via the Grotthuss mechanism through an extended network of hydrogen bonds. This mechanism ensures proton conductivity in the absence of moisture. Polybenzimidazole can be doped with many inorganic acids, but phosphoric acid is most often used owing to its good thermal stability and low vapor pressure [105, 107–114]. Electroconductivity of the PBI membrane doped with phosphoric acid depends on temperature and the doping level, being up to 140 mS/cm at 160°C [115]. However, pyrolysis of phosphoric acid at temperature above 90°C, corrosion

Table 1. Composition of PBI-based membranes, relative humidity *RH*, specific electroconductivity κ, and decomposition temperature T_{dec}

Membrane	*RH*, %	*T*, °C	κ, mS/cm	T_{dec}, °C	Application	Reference
Polymer + ionic liquid (wt %)						
PBI–DEMA/TfO (1, 2, 3, 4)[a]	10–40	60–90	0.1 (80°C)	435	Fuel cell	[85]
PBI–DEMA/TfO (37.5–60%)	AH	100–250	108.9 (250°C)	310	″	[86]
PBI–DEMA/TfO (33–83%)	AH	40–160	20.73 (160°C)	230	″	[87]
PBI–DEMA/TFSI (1, 2)[a]	AH	80–180	0.3 (180°C)	250	″	[88]
PBI–DEA/HSO_4 (3–12)[a]	0–16	25–200	30 (160°C)*	200	″	[89]
PBI–SEMA/TfO (1.5)[a]	30	100	2.68	380	″	[90]
PBI–MIm/TFSI (37.5–60%)	AH	100–250	45 (250°C)*	335	″	[86]
PBI–EMIm/TfO (37.5–60%)	AH	100–250	46 (250°C)*	336	″	[86]
PBI–BIm/TfO (1.35, 2.2, 3.2)[a]	AH	30–145	1.55 (145°C)	180	″	[91]
PBI–OHEMIm/TFSI (37.5–60%)	AH	100–250	50 (250°C)*	383	″	[86]
PBI–BMIm/Cl (5%)	9**	20–200	0.1 (160°C)	300	Electroconductive membrane	[92]
PBI–BMIm/BF_4 (5%)	7**	20–200	2×10^{-3} (200°C)	300	″	[92]
PBI–BMIm/TFSI (5%)	9**	20–200	0.65 (160°C)	300	″	[92]
PBI–BMIm/NCS (5%)	8**	20–200	3×10^{-4} (200°C)	300	″	[92]
PBI–HMIm/TfO (2, 3, 4)[a]	AH	80–250	16 (250°C)	348	Fuel cell	[93]
PBI–MIm/TFSI (N)	AH	130–190	1.86 (190°C)	300	″	[94]
(PBI/ETS)–MIm/TFSI (73%)	AH	20–200	0.15 (180°C)		″	[95]
(PBI+SPEEK)–TESPA/HSO_4 (2.5, 5%)	60–100	25, 80	101 (80°C)	290	″	[96]
(PBI+SPEEK)–BIm/HSO_4 (2.5, 5%)	60–100	25, 80	94 (80°C)	355	″	[96]
(PBI–O–Ph)–EIm/TfO (40, 50, 70%)	N	25–160	5 (160°C)*		″	[97]
(PBI–O–Ph)–BMIm/TfO (40, 50, 70%)	N	25–160	2.35 (140°C)*		″	[97]

Table 1. (Contd.)

Membrane	*RH*, %	*T*, °C	κ, mS/cm	T_{dec}, °C	Application	Reference
Polymer + ionic liquid + acid						
[PBI–DEMA/TFSI (1, 2)][a]–H_3PO_4(1–9)[a]	5	80–180	60 (180°C)	200	Fuel cell	[88]
[PBI–MDA (0-2%)]–$Pr(MIm)_2Br_2$ (4.5%)–H_3PO_4 (11–15%)	AH	25–180	224 (180°C)	180	″	[98]
[pPBI–MsMIm/Cl (5–20%)]–H_3PO_4 (N)	AH	110–170	103 (170°C)	250	″	[99]
[PBI–BMIm/Cl (5%)]–H_3PO_4 (60%)	AH	0–200	26 (200°C)	180–210	″	[100]
[PBI–BMIm/Br (5%)]–H_3PO_4 (60%)	AH	0–200	58 (200°C)	180–210	″	[100]
[PBI–BMIm/I (5%)]–H_3PO_4 (60%)	AH	0–200	68 (200°C)	180–210	″	[100]
[PBI–BMIm/BF_4 (5%)]–H_3PO_4 (60%)	AH	0–200	94 (200°C)	180–210	″	[100]
[PBI–BMIm/PF_6 (5%)]–H_3PO_4 (60%)	AH	0–200	23 (200°C)	180–210	″	[100]
[PBI–BMIm/NCS (5%)]–H_3PO_4 (60%)	AH	0–200	26 (200°C)	180–210	″	[100]
[PBI–BMIm/TFSI (5%)]–H_3PO_4 (60%)	AH	0–200	65 (200°C)	180–210	″	[100]
[PBI/IPTS–BMIm/H_2PO_4 (3–10%)]–H_3PO_4 (8–10)[a]	AH	100–170	133 (160°C)	160–250	″	[101]
PBI–ApMIm/Br-GO (5)–H_3PO_4 (2, 3.5)[a]	AH	100–180	35 (175°C)	N	″	[102]
PBI–[NH_4BEA + MtOHTMA/$(CH_3)_2PO_4$ (29%)](3, 10, 20%)–H_3PO_4 (3.1, 3.4, 5.9)[a]	100, 0.05**	RT–200	65 (100°C) 5 (100°C)	20–200	″	[103]
PBI–[NH_4BEA+DMEtOHA/TFSI (5%)](3, 10, 20%)–H_3PO_4 (1.6, 3.4, 5.9)[a]	100, 0.05**	RT–200	61 (100°C) 0.15 (100°C)	20–200	″	[103]
PBI–[NaY+DMEtOHA/TFSI (17%)] (3, 10, 20%)–H_3PO_4 (8.5, 8.9, 12.1)[a]	100, 0.05**	RT–200	34 (100°C) 6 (100°C)	20–200	″	[103]
PBI–[NaY+MIm/TFSI (19%)] (3, 10, 20%)–H_3PO_4 (4.6, 8.7, 12.0)[a]	0.05**	RT–200	32 (150°C)	20–200	″	[103]
(PBI/ETS)–MIm/TFSI (35%)–H_3PO_4 (40%)	AH	20–200	10 (170°C)	20–200	″	[95]

RT: room temperature, AH: anhydrous conditions, FH: full hydration.
[a] Number of moles of ionic liquid–acid per 1 mol of the repeat unit of PBI.
N: not stated.
* The value taken from the plot.
**Absorption, %.

of the catalyst, leaching of the acid, and deterioration of the mechanical properties during the operation lead to decrease in the membranes electroconductivity. To improve the mechanical properties and increase electroconductivity of the PBI–H_3PO_4 membrane, the polymer matrix can be doped with ionic liquid. If the ionic liquid is protic, it can be also involved in the proton transfer. For example, the PBI–DEMA/TFSI polymer composite membrane with the ionic liquid : polybenzimidazole molar ratio 1 and 2 was obtained and further incorporated with H_3PO_4 [88]. The ionic liquid acted as plasticizer in the obtained membranes, making them more flexible and preventing the acid leakage from the membrane. To confirm the efficiency of the obtained membrane in a fuel cell, they were tested in the membrane electrode assembly. The highest specific power was achieved at 200°C, being 0.32 W/cm^2 at 900 mA/cm^2.

The (PBI–ionic liquid)–H_3PO_4 membranes were prepared similarly in [100] using the salts with the 1-butyl-3-methylimidazolium (BMIm) cation and different anions as the ionic liquid, its content in the membrane being 5 wt %. The effects of the anion (Cl, Br, I, NCS, TFSI, PF_6, and BF_4) on structure, morphology, thermal, oxidative, and mechanical stability, and proton conductivity of the membranes were analyzed. The considered (PBI–ionic liquid)–H_3PO_4 membranes exhibited increased thermal, oxidative, and mechanical stability in comparison with the PBI–H_3PO_4 membrane. Electroconductivity of the membranes containing 5 wt % of BMIm/Cl and BMIm/I was lower in comparison with the PBI–H_3PO_4 membrane, whereas that of the membranes containing other probed salts was lower in comparison with the membrane doped only with phosphoric acid.

The (PBI–ionic liquid)–H_3PO_4 membranes containing dication (1,3-di(3-methylimidazolium)propane bis(trifluoromethylsulfonyl)imide and 1,6-di(3-methylimidazolium)hexane bis(hexafluorophosphate)) and monocation (1-hexyl-3-methylimidazolium bis(trifluoromethylsulfonyl)imide and 1-butyl-3-methylimidazolium hexafluorophosphate) ionic liquids were compared in [116, 117]. The membranes containing the dication as well as monocation ionic liquids were found more thermally stable and revealed higher electroconductivity in comparison with the PBI–H_3PO_4 membrane; at the same time, electroconductivity of the membranes with the dication ionic liquids was higher than that for the membranes with the monocation ionic liquids. The performed testing of the membranes containing ionic liquids in the membrane electrode assembly revealed that they outperformed the PBI–H_3PO_4 membrane. That fact was mainly related to higher electroconductivity of the (PBI–ionic liquids)–H_3PO_4 membranes as well as plasticizing effect of the ionic liquids, resulting in the improved contact of the membrane with the cathode and anode.

Modified polybenzimidazole or inorganic filler functionalized with ionic liquid was used to improve the properties of proton-conducting membranes. Modification of polybenzimidazole was performed in [101] to prevent the leakage of 1-butyl-3-methylimidazolium dihydrophosphate (BMIm/H_2PO_4) and H_3PO_4 from the (PBI–ionic liquid)–H_3PO_4 composite membrane and to improve its mechanical properties. To do so, hydroxyl-bearing polybenzimidazole was prepared, which further interacted with 3-(triethoxysilyl)propyl isocyanate (IPTS). The membranes produced of such modified PBI (cPBI in Fig. 2) possessed the cage-like cross-linked structure formed via the hydrolysis reaction due to the Si–O–Si crosslinking. Other conditions being the same, electroconductivity of the membranes containing BMIm/H_2PO_4 (5, 8, or 10 wt %) was higher in comparison with the PBI–H_3PO_4 membranes. Two paths of the proton transfer are possible in the (PBI–ionic liquid)–H_3PO_4 membranes: hopping of protons between the molecules of H_3PO_4 and the imidazole rings of PBI (blue path in Fig. 2) and the proton transfer between the molecules of H_3PO_4, BMIm/H_2PO_4, and imidazole rings of PBI (rose path in Fig. 2). The ionic liquid captured in the case favored the absorption of H_3PO_4 and acted as the protons acceptor, thus shortening the distance of the proton transfer and enhancing the proton conductivity.

Modified polybenzimidazole was also used in [95] to produce the membrane. Porous PBI membrane was first prepared, and then linking of the hydroxyl groups of the titanosilicate microporous material ETS-10 and the amino groups of polybenzimidazole afforded the ETS-10 "grafting" at polybenzimidazole. The described reaction was performed using functionalized ETS-10 prepared via the interaction with 3-(2,3-epoxypropoxy)propyltrimethoxysilane. A deal of attention was paid in that study to the effect of the order of the stages of polybenzimidazole functionalization and the membrane doping with phosphoric acid and ionic liquid (MIm/TFSI) on the membrane electroconductive properties. Hydrophilic nature of MIm/TFSI ensured absorption of water from the gas phase, suppressed oligomerization of phosphoric acid, and changed the conductivity profile at temperature above 160°C. ETS-10 covalently linked to polybenzimidazole prevented leakage of the proton conductor from the membrane and at the same time suppressed the crossover of the fuel H_2 and methanol.

In [103], ionic liquids (2-hydroxymethyltrimethylammonium dimethylphosphate, *N*,*N*-dimethyl-*N*-(2-hydroxyethyl)ammonium bis(trifluoromethylsulfonyl)imide, and 1-H-3-methylimidazolium bis(trifluoromethylsulfonyl)imide) were incorporated in the zeolites (NH_4BEA and NaY), and their influence on the degree of doping of the PBI membranes with

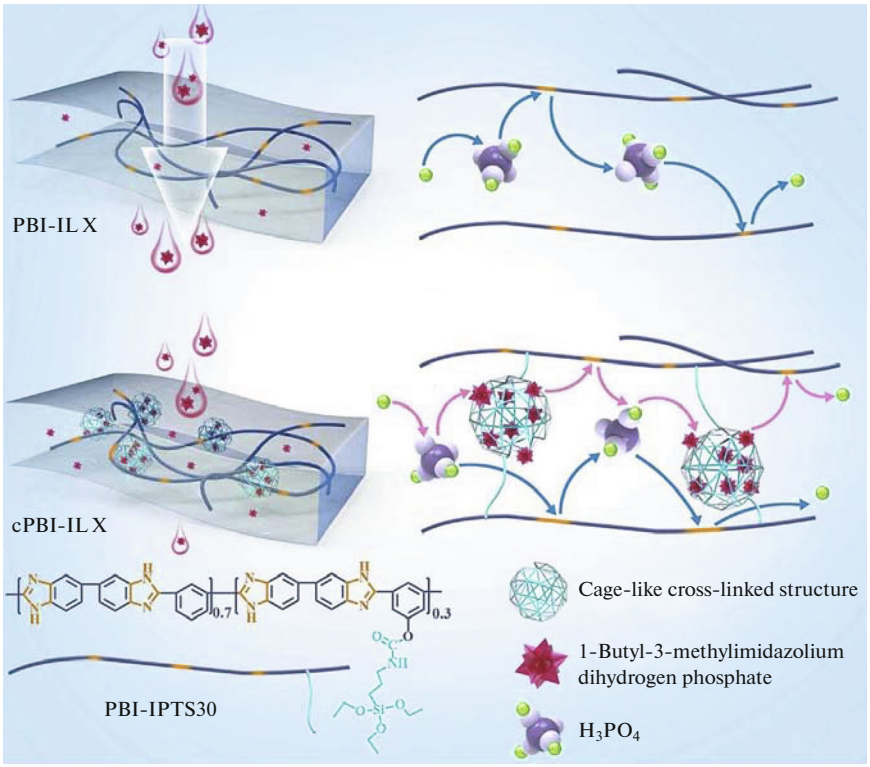

Fig. 2. Possible paths of proton transport in the membranes. Reproduced with permission from [101].

phosphoric acid, their morphological, physico-chemical, and electrochemical properties was elucidated. The membranes containing MIm/TFSI–NaY were found the best of the tested membranes. Conductivity and selectivity of the H^+/H_2 transport by the PBI–[NaY–MIm/TFSI]–H_3PO_4 membranes exceeded those characteristics of the PBI–H_3PO_4 and PBI–NaY–H_3PO_4 membranes. The authors related the obtained result to the presence of the presence of the MIm cations and the TFSI anions at the NaY surface, capable of the acid-base interactions with the components of the PBI–H_3PO_4 system and involved in the proton transfer via the Grotthuss mechanism. The produced membrane also exhibited good operational properties during the test in the membrane electrode assembly.

Composite membrane with graphene oxide functionalized with ionic liquid (ILGO) as the filler was prepared in [102]. The (PBI–ILGO)–H_3PO_4 membrane exhibited high electroconductivity at low content of phosphoric acid, which prevented its leakage, favoring the membrane use in fuel cells. The fuel cell with the (PBI–ILGO)–H_3PO_4 membrane exhibited maximum specific power 320 mW/cm^2 at 175°C, which exceeded that of the fuel cell with the PBI–H_3PO_4 membrane.

The (PBI–ionic liquid)–H_3PO_4 membrane for flexible supercapacitor has was prepared in [99] using porous polybenzimidazole and (1-(3-trimethoxysilylpropyl)-3-methylimidazolium chloride (MsMIm/Cl). The ionic liquid in the polymer matrix (PBI–ionic liquid) was subject to hydrolysis with the formation of the Si–O–Si bonds. Electroconductivity of the composite membrane was up to 103 mS/cm at 170°C; it exhibited good mechanical properties and thermal stability. The high value of electroconductivity was owing to porous structure of the polymer matrix, ensuring higher absorption of H_3PO_4. Moreover, the ionic liquid acted as the proton carrier, allowing effective increase in the proton conductivity. The produced supercapacitor with such membrane retained stable electrochemical parameters under conditions of bending, its specific capacity being up to 85.5 F/g at 120°C, 3 times higher than at room temperature.

Summarizing the above-said, introduction of a ionic liquid in the PBI-acid polymer membrane can improve the mechanical properties of the membranes and enhance their thermal stability and electroconductivity (up to 10^{-1} S/cm).

(PBI–Ionic Liquid) Polymer Electrolyte

The promises of the application of protic ionic liquids as the proton donor in the proton-conducting membranes have been discussed in a series of studies [62, 69, 71, 85, 86, 91].

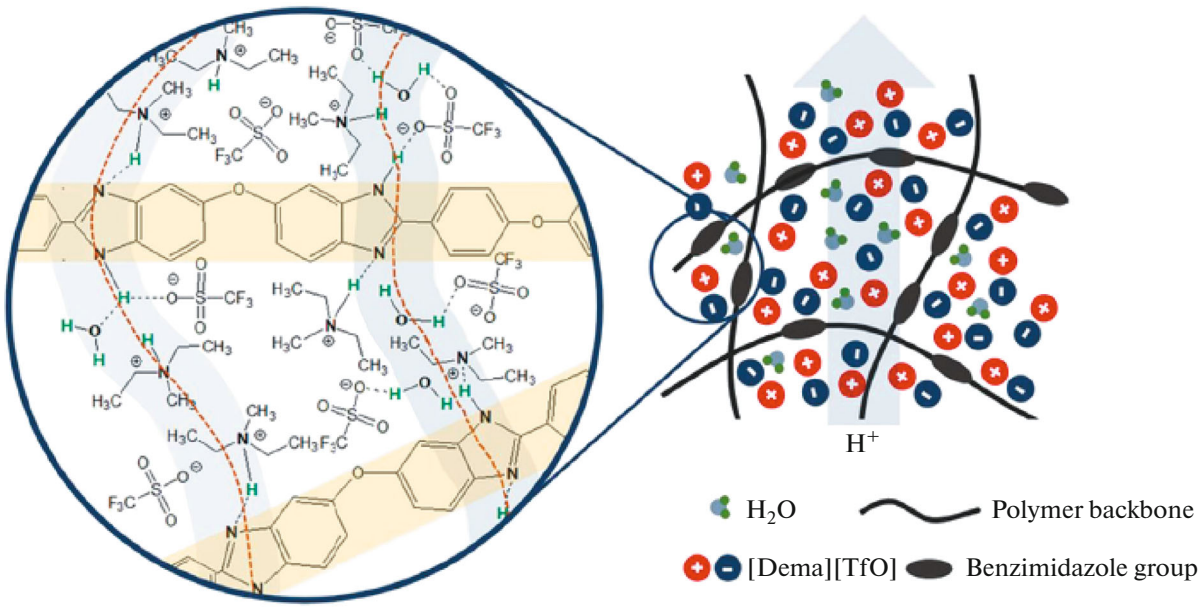

Fig. 3. Proton transport in the PBI–DEMA/TfO membrane. Reproduced with permission from [85].

Commercially available diethylmethylammonium triflate (DEMA/TfO) is the best studied protic ionic liquid for preparation of the PBI-based membranes. The PBI–DEMA/TfO membranes containing 1 to 4 mol of DEMA/TfO per a repeat unit of PBI were produced in [85]. Basing on the IR and NMR spectroscopy data, weak interaction of the cations and anions of DEMA/TfO with the imidazole fragments of PBI was observed. Thermal stability of the membranes was also discussed in detail in the report. The mass loss at 250°C in the TGA curve was related to elimination of the excess (free) DEMA/TfO and diethylmethylamine due to the protonation of PBI with the formation of $(PBI\text{-}H_2^+)_x\cdot(CF_3SO_3^-)_{2x}$, that at 380°C was assigned to elimination of TfOH via decomposition of $(PBI\text{-}H_2^+)_x\cdot(CF_3SO_3^-)_{2x}$, and finally that at 500°C marked complete decomposition of PBI into CO_2, N_2, hydrocarbons, and carbonaceous residue. The influence of residual water which could be accumulated during the fuel cell operation was studied. It was shown that the increase in the relative humidity from 10 to 40% led to the increase in the PBI–DEMA/TfO membrane electroconductivity by an order of magnitude.

Using the model system consisting of a mixture of DEMA/TfO and the benzimidazole monomer (BIm instead of the polymer PBI), the proton transfer mechanism was studied by means of ^{1}H NMR and NMR with pulsed field gradient. In the absence of water, fast proton exchange between NH^+_{DEMA} and NH_{BIm} was observed. In the presence of water, the conductivity in the model system was due to the cooperative mechanism involving all the species (NH^+_{DEMA}, NH_{BIm}, and H_2O), which accelerated the proton transfer. Basing on the obtained data, the model of the proton transfer in the PBI–DEMA/TfO membrane was suggested (Fig. 3).

The membranes for the H_2/Cl_2 fuel cells based on PBI doped with DEMA/TfO were also investigated in [87]. The content of the ionic liquid in the membrane ranged between 33 and 83%. Basing on the IR spectroscopy data, it was concluded that the increase in the DEMA/TfO concentration led to the interaction between the C=N group in PBI and the N–H group of the ammonium cation, resulting in protonation of the imide group of imidazole. The DSC thermograms of the membranes containing less than 67% of DEMA/TfO did not reveal endothermic peaks related to melting of free DEMA/TfO. However, the presence of small amount of free ionic liquid in the PBI membrane was observed with further increase in the content of DEMA/TfO. The membranes with high content of DEMA/TfO exhibited electroconductivity up to $>10^{-3}$ S cm^{-1} at 40°C. The so high values of electroconductivity were related to the increase in the ionic mobility as well as the formation of the developed ionic channels. Low values of the electroconductivity activation energy ($\Delta G_\kappa^{\neq}$), of 14–27 kJ/mol, pointed at the predominance of the Grotthuss mechanism of the proton transfer in those membranes. At the same time, at high concentration of the ionic liquid in the membrane, in the presence of free DEMA/TfO, the proton transfer can also occur via the transport mechanism. Figure 4 displays the suggested hypothesis on the ionic electroconductivity. The H_2/Cl_2 fuel cell with the

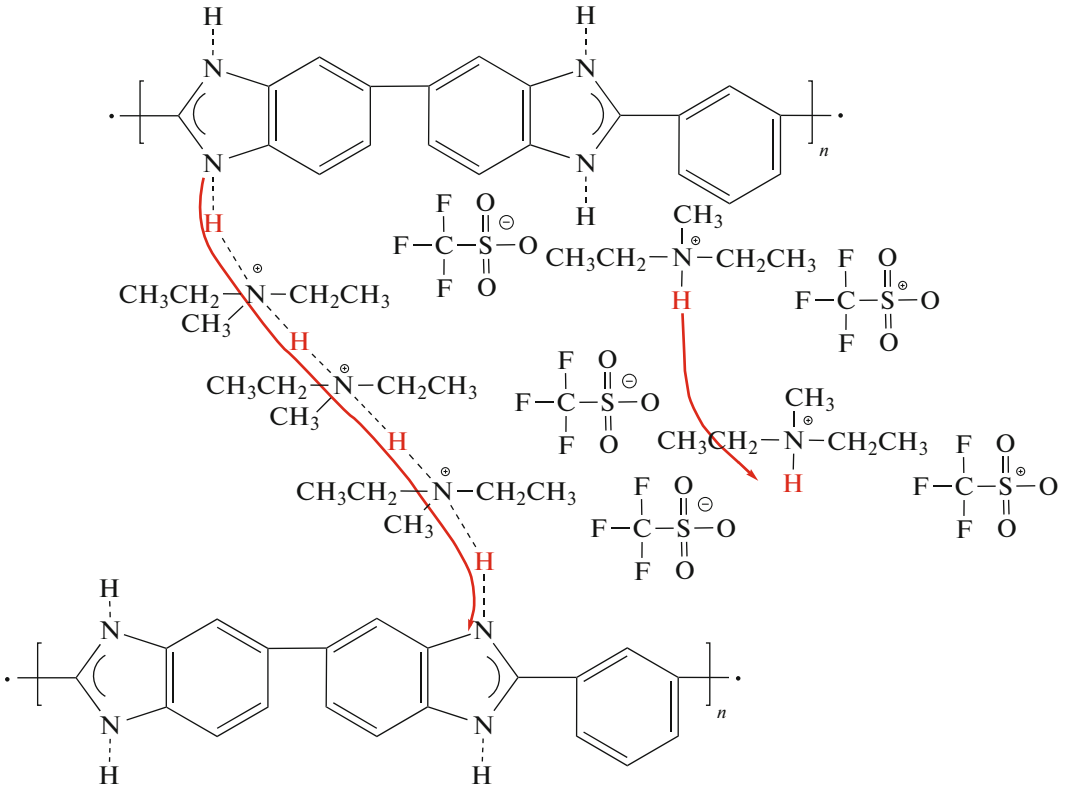

Fig. 4. Hypothesis on ionic conductivity in the PBI–DEMA/TfO membrane. Reproduced with permission from [87].

PBI–DEMA/TfO membrane containing 83% of DEMA/TfO exhibited specific power of 26.50 and 29.64 mW/cm^2 at 120 and 140°C, respectively.

The membranes produced of PBI and several ionic liquids: diethylmethylammonium trifluoromethanesulfonate (DEMA/TfO), 1-ethyl-3-methylimidazolium trifluoromethanesulfonate (EMIm/TfO), 1-methylimidazolium bis(trifluoromethanesulfonyl)imide (MIm/TFSI), and 1-(2-hydroxyethyl)-3-methylimidazolium bis(trifluoromethanesulfonyl)imide (OHEMIm/TFSI) were studied in [86]. Qualitative analysis of the membranes chemical structure basing on the IR spectra revealed that DEMA/TfO, MIm/TFSI, and OHEMIm/TFSI formed hydrogen bonds with the polymer, whereas EMIm/TfO was physically adsorbed at PBI and did nor form the H-bonds. Temperature dependences (100–250°C) of electroconductivity of different membranes studied in [86] are shown in Fig. 5.

The calculated values of the activation energy of electroconductivity were of 16.0 to 26.8 kJ/mol, hence it was concluded that the proton transfer occurred via the Grotthuss mechanism (typical $\Delta G_к^{\neq}$ values 14–40 kJ/mol).

The membranes based on PBI doped via swelling in a highly acidic protic ionic liquid, 2-sulfoethylmethylammonium trifluoromethanesulfonate (SEMA/TfO), were studied in [90]. The interaction of the acidic cations of the ionic liquid with basic groups of the polymer led to their protonation with the formation of neutral molecules of *N*-methyltaurin. Furthermore, fast proton exchange between the acidic cation SEMA and water molecules was observed. As a result, the proton conductivity occurred via the transport mechanism with the protic ionic liquid cation and H_3O^+ as well as via the cooperative mechanism involving both types of the ions. The electroconductivity of the obtained membranes was weak, due to low level of the polymer doping. The degree of absorption of the protic ionic liquid with polybenzimidazole via swelling depended on the cation acidity: lower acidity of the cation led to lower swelling degree. Despite certain features of such membranes, the authors concluded that protic ionic liquids possessing high Brønsted acidity were promising candidates for the application as nonaqueous electrolytes.

The influence of the nature of the anion (Cl, NCS, TFSI, BF_4) in the ionic liquid with the BMIm cation on electroconductivity of the PBI–ionic liquid polymer membrane was discussed in [92]. The values of the electroconductivity activation energy depending on the anion nature followed the $\Delta G_к^{\neq}(\text{TFSI}) < \Delta G_к^{\neq}(\text{Cl}) < \Delta G_к^{\neq}(\text{BF}_4) < \Delta G_к^{\neq}(\text{NCS})$ series. They were

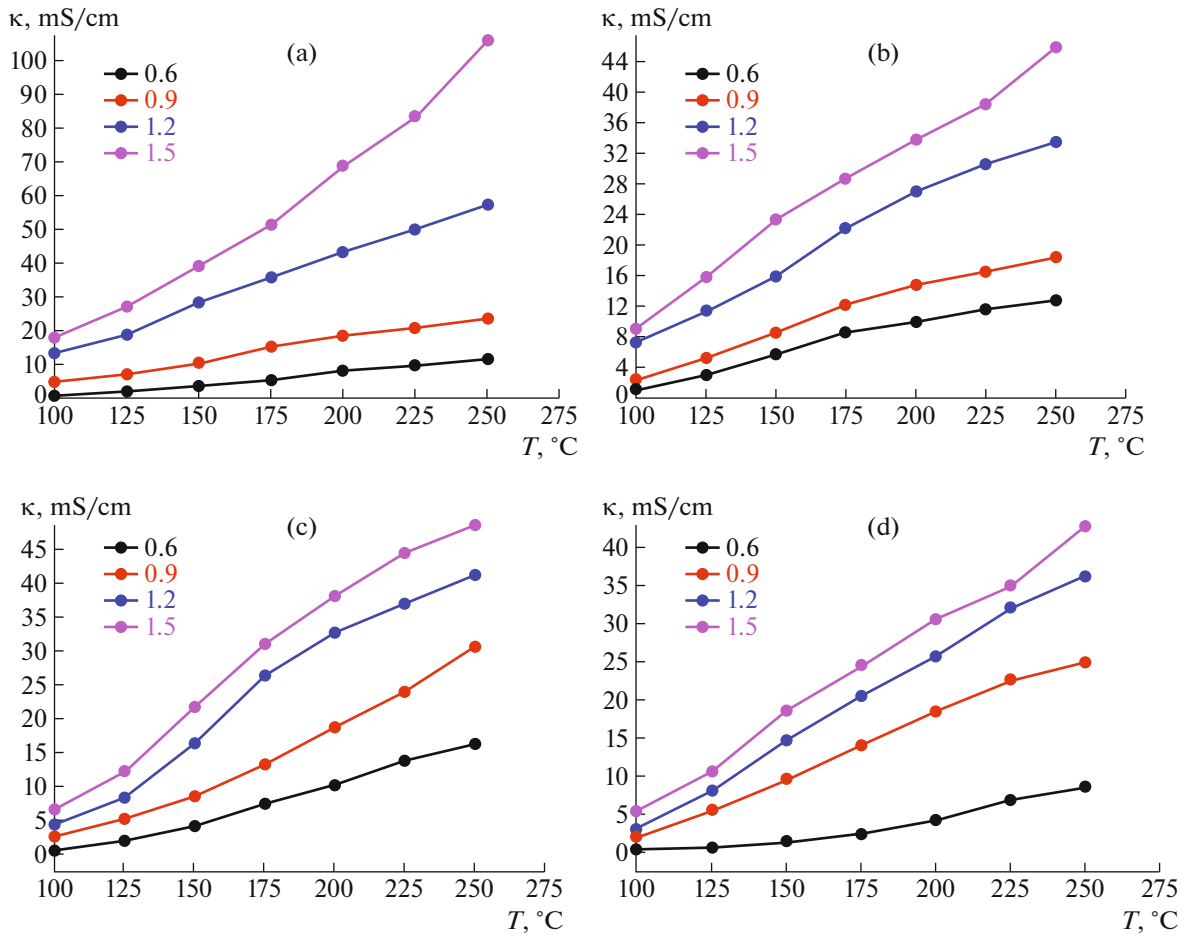

Fig. 5. Temperature dependence of specific electroconductivity of anhydrous PBI–ionic liquid membranes with different content of the ionic liquid: DEMA/TfO (a), EMIm/TfO (b), OHEMIm/TFSI (c), and MIm/TFSI (d). Mass ratio PBI : ionic liquid = 1.0 : 0.6, 1.0 : 0.9, 1.0 : 1.2, 1.0 : 1.5. Reproduced with permission from [86].

of 65–84 kJ/mol, suggesting the transport mechanism of the ionic transfer.

The PBI–BIm/TfO proton-conducting membranes with different molar ratios of the IL and polymer units (1.35/1, 2.2/1, 3.2/1) were obtained in [91]. Their phase behavior as well as thermal and electrochemical stability were studied, and the specific electroconductivity was measured over a wide temperature range. The DSC study performed over the −80... +150°C range revealed that no phase transitions typical of pure BIm/TfO were observed in the case of the membrane. The membranes electroconductivity was increased with the increase in the ionic liquid content, yet remained lower in comparison with pure *N*-butylimidazolium trifluoromethanesulfonate.

In conclusion to this section, let us notice that since specific electroconductivity of polymer proton-conducting membranes above 10^{-2} S/cm is considered sufficient for fuel cells application [118], analysis of electroconductivity of the PBI–ionic liquid membranes (Table 1) has revealed that such membranes can be competitive to the Nafion membranes. The use of protic ionic liquid as proton conductor in the PBI membrane can significantly extend temperature range of the fuel operation towards high-temperature range in comparison with the PBI–acid membranes.

Polymer Electrolytes Based on Poly(Vinylidene Fluoride-co-Hexafluoropropylene)

Poly(vinylidene fluoride-*co*-hexafluoropropylene)

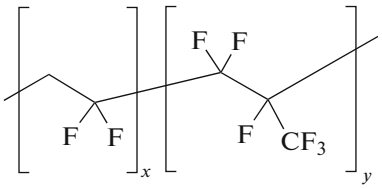

is a common fluorinated copolymer widely used as polymer matrix, due to its high thermal and chemical resistance, hydrophobicity, and ability to retain liquid electrolytes in the derived membranes.

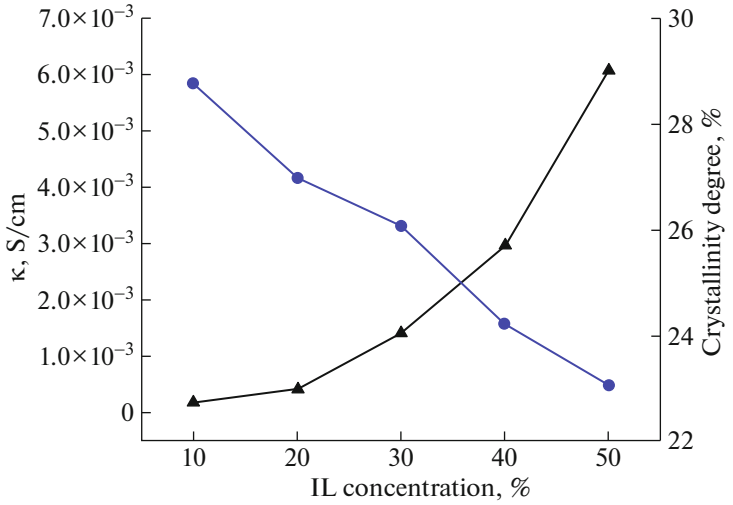

Fig. 6. Electroconductivity and degree of crystallinity of the (PVdF–HFP)–BMIm/Br polymer electrolyte as functions of the ionic liquid (IL) concentration. Reproduced with permission from [2].

PVdF–HFP is a semicrystalline polymer, i.e., a mixture of amorphous of crystalline regions. Crystalline vinylidene fluoride units ensure structural integrity allowing the formation of free-standing films, whereas the units of amorphous hexafluoropropylene aid in ionic species retention. The (–C–F) groups in PVdF–HFP act as electron acceptors ensuring the anodic stability. The PVdF–HFP copolymer also exhibits high solubility in organic solvents, which is very important as far as the solution casting method of the membranes preparation is concerned. Table 2 lists the reference data on the composition and selected properties of polymer electrolytes based on PVdF–HFP and ionic liquids.

Among the electrochemical devices, the (PVdF–HFP)–ionic liquid polymer electrolytes have been most widely applied in capacitors and in the production of polymer electrolyte membranes for batteries, where the ionic liquid is often used as solvent for lithium/sodium salts.

As has been shown in many studies [2, 119, 123, 129, 135, 139, 141, 142, 144, 145, 151, 170, 175], the interaction of the ionic liquid with polar $-CF_3$ groups of PVdF–HFP leads to significant conformational changes in the polymer, resulting in the decreased degree of crystallinity and, consequently, increase in electroconductivity. For example, the correlation between the change in conductivity and degree of crystallinity of PVdF–HFP depending on the concentration of 1-butyl-3-methylimidazolium bromide (BMIm/Br) (Fig. 6) was observed in [2].

(PVdF–HFP)–Ionic Liquid Polymer Electrolyte

Since the (PVdF–HFP)–ionic liquid polymer electrolytes are mainly applied in supercapacitors, aprotic ionic liquids are most often used in such electrolytes.

It has been shown in many studies that increase in the ionic liquid concentration leads to increase in electroconductivity of the (PVdF–HFP)–ionic liquid polymer electrolyte until certain threshold and can be decreased with further increase in the ionic liquid content. For example, in [134] it was demonstrated that the increase in the BMIm/I content led to increase in the conductivity of the (PVdF–HFP)–ionic liquid electrolyte due to the increase in the number of the ionic species, to reach the limiting value of 3.9 mS/cm at the BMIm/I : (PVdF-HFP) mass ratio of 4 : 1. However, further increase in the ionic liquid content led to decrease in the ionic conductivity due to the ionic aggregation (Fig. 7a).

The addition of 1-ethyl-3-methylimidazolium bromide (EMIm/Br) (~10 wt %) to the PVdF–HFP polymer also resulted in the system conductivity increase to 4.82×10^{-3} S/cm at the ionic liquid concentration of 70 wt %, remaining practically constant with further increase in the concentration of EMIm/Br [140] (Fig. 7b).

Polymer electrolyte films based on PVdF–HFP with different contents of the 1-ethyl-3-methylimidazolium tricyanomethanide (EMIm/TCM) ionic liquid were prepared in [129]. Ionic conductivity of the polymer electrolyte films was increased with the increase in the content of the ionic liquid in the polymer, up to the highest value of 37 mS/cm at the doping degree of 300 wt %, which exceeded the electroconductivity of the pure ionic liquid. It was found that the films containing up to 400 wt % of the ionic liquid were mechanically stable, but at higher concentration

Table 2. Composition of membranes based on PVdF–HFP, relative humidity *RH*, specific electroconductivity κ, and decomposition temperature T_{dec}

Membrane	*RH*, %	*T*, °C	κ, mS/cm	T_{dec}, °C	Application	Reference
Polymer + ionic liquid (wt %)						
(PVdF-HFP)–EMIm/BF_4 (75%)	N	−60–40	16.8 (30°C)		Electrochemical double layer capacitor	[119]
[(PVdF-HFP)–EMIm/BF_4 (75%)]+ZnO (5%)	N	−60–40	2.57 (30°C)		″	[119]
[(PVdF-HFP)–EMIm/BF_4 (75%)]+TiO_2 (5%)	N	−60–40	3.75 (30°C)		″	[119]
(PVdF-HFP)–EMIm/BF_4 (75%)	N	25–65	8.6 (RT)		Supercapacitor	[120]
(PVdF-HFP)–EMIm/BF_4 (90%)	N	RT	25		Microsupercapacitor	[121]
(PVdF-HFP)–BMIm/BF_4 (80%)	AH	−30–80	1.79 (20°C)	250–350	Supercapacitor	[122]
(PVdF-HFP)–BMIm/BF_4 (25–75%)–SN (25–75%)	AH	−30–80	6.4 (20°C)	250–350	″	[122]
(PVdF-HFP)–EMIm/TFSI (85%)	AH	RT	3.3	350	″	[123]
(PVdF-HFP)–EMIm/TFSI (96%)	>50 ppm	25–100	8.6 (25°C)		″	[124]
(PVdF-HFP)–EMIm/TFSI (75%)	N	25	0.95	333	″	[125]
(PVdF-HFP)–EMIm/TFSI(75%)–LASGP (9%)	N	25	5.22	346	″	[125]
(PVdF-HFP)–EMIm/TFSI (83%)	AH	RT	11	300	″	[126]
[(PVdF-HFP)–EMIm/TFSI(83%)]–GO (1%)	AH	RT	25	300	″	[126]
[(PVdF-HFP)/TAIC (5%)]–EMIm/TFSI (75%)	N	RT	1.4	420	Electrochemical device	[127]
(PVdF-HFP)/P(MMA-*co*-BMA)–EMIm/TFSI (70%)	N	−40–80	1.02 (RT)	300	″	[3]
[(PVdF-HFP)–GNSs (0.03–0.3%)]–EMIm/TFSI (80%)	N	RT	6.7	400	Supercapacitor	[128]
(PVdF-HFP)–EMIm/TCM (9–82%)	N	RT	37.6	261	Electrochemical device	[129]
(PVdF-HFP)–EMIm/TfO (80%)	N	20–100	5.2 (RT)		Sodium-sulfur battery	[130]
(PVdF-HFP)–EIm/TfO(60%)	0–22	20–160	85 (90°C, RH)* 5 (140°C, AH)*		Fuel cell	[131]
(PVdF-HFP)–EMIm/TCB (80%)	AH	20–90	9 (RT)	310	Supercapacitor	[132]
(PVdF-HFP)–BMIm/TfO (40, 50, 70%)	N	25–160	19 (160°C)		Fuel cell	[90]
(PVdF-HFP)–BMIm/TfO (60%)	0–22	20–160	18 (140°C, RH)* 17 (160°C, AH)*		″	[131]
(PVdF-HFP)–BMIm/TFSI (20–80%)	AH	30–160	0.66 (RT)	300–350	Rechargeable battery	[133]
(PVdF-HFP)–BMIm/I (2–5) [a]	N	RT	4		Supercapacitor	[134]
(PVdF-HFP)–BMIm/Br (10–50%)	N	25–90	6.3 (RT)	235–325	Electrochemical device	[2]
(PVdF-HFP)–BMIm/NCS (40%)	N	25–100	0.15 (RT)		Lithium-ion battery	[135]

Table 2. (Contd.)

Membrane	*RH*, %	*T*, °C	κ, mS/cm	T_{dec}, °C	Application	Reference
(PVdF-HFP)–BMIm/Cl (50–80%)	N	30–90	4.1 (30°C) 15 (90°C)		Electrochemical double layer capacitor	[136]
[(PVDF-HFP)+PVP]–BMIm/HSO_4 (50–70%)	60	30–130	3.9 (30°C)		Fuel cell	[137]
(PVdF-HFP)–BMIm/Cl (60%)–(1M TetEA/BF_4 in EC/PC(1 : 1)) (20%)	N	30–100	8.9 (30°C)		Electrochemical double layer capacitor	[138]
(PVdF-HFP)–BMIm/BF_4 (10–90%)	N	30–90	5.9 (30°C)	300–400	Electrochemical device	[139]
[(PVdF-HFP)–BMIm/I (4)[a]] + CNTs (1×10^{-3}–4×10^{-3})[a]	N	RT	17.6		Supercapacitor	[134]
(PVdF-HFP)–EIm/TfO (40, 50, 70%)	N	25–160	9.5 (100°C)		Fuel cell	[97]
(PVdF-HFP)–EMIm/Br (10–80%)	N	RT	4.82		Supercapacitor	[140]
(PVdF-HFP)–AEIm/TFSI (33.3–85.7%)	N	RT	0.052		Electrochemical double layer capacitor	[141]
(PVdF-HFP)–AMIm/TFSI (33.3–85.7%)	N	RT	0.029		Electrochemical double layer capacitor	[141]
(PVdF-HFP)–AMEtIm/TFSI (33.3–85.7%)	N	RT	0.039		″	[141]
(PVdF-HFP)–DMEA/TFA (0.005) [b]	AH	50, 100	2.1 (50°C)	190	Electrochemical device	[142]
(PVdF-HFP)–DEA/TFA (0.005) [b]	AH	50, 100	2.97 (50°C)	212	″	[142]
(PVdF-HFP)–TEA/TFA (0.005) [b]	AH	50, 100	1.76 (50°C)	186	″	[142]
(PVdF-HFP)–TEOA/TFA (0.005) [b]	AH	50, 100	1.02 (50°C)	203	″	[142]
(PVdF-HFP)–DIPEA/TFA (0.005) [b]	AH	50, 100	1.68 (100°C)	194	″	[142]
(PVdF-HFP)–TBA/TFA (0.005) [b]	AH	50, 100	0.36 (50°C)		″	[142]
(PVdF-HFP)–AMEtA/TFSI (33.3–85.7%)	N	RT	0.13		Electrochemical double layer capacitor	[141]
(PVdF-HFP)–MMEtA/TFSI (33.3–85.7%)	N	RT	0.145		″	[141]
((PVdF-HFP)+Nafion) (32%)+SWCNT (20%)–DEMMsA/BF_4 (48%)	N	RT	0.17		Energy conversion devices	[1, 143]
((PVdF-HFP)+Nafion) (32%)+SWCNT (20%)–DEMMsA/CF_3BF_3 (48%)	N	RT	0.16		″	[1, 143]
((PVdF-HFP)+Nafion) (32%)+SWCNT (20%)–DEMMsA/$C_2F_5BF_3$ (48%)	N	RT	0.07		″	[1, 143]
((PVdF-HFP)+Nafion) (32%)+SWCNT (20%)–DEMMsA/TFSI (48%)	N	RT	0.11		″	[1, 143]
Polymer + ionic liquid + acid						
(PVdF-HFP)–DEMA/TfO (0–80%)–H_3PO_4 (40%)	AH	RT	0.63	100–200	Fuel cell	[144]
(PVdF-HFP)–DEMA/TfO(10–80%)–$HClO_4 \cdot SiO_2$(N)	AH	RT, 100	0.6 (100°C)		Fuel cell, supercapacitor	[145]

Table 2. (Contd.)

Membrane	*RH*, %	*T*, °C	κ, mS/cm	T_{dec}, °C	Application	Reference
Polymer + ionic liquid + Li(Na) salt						
[(PVdF-HFP)–EMIm/TfO (80%)]–(0.5M Na/TfO in EMIm/TfO)	N	20–100	5.7 (RT)		Sodium-sulfur battery	[130]
((PVdF-HFP)+TiO_2)–(0.5M Na/TfO in BMIm/TfO)	AH	35–80	0.4 (RT)		″	[146]
(PVdF-HFP)–(0.5M Na/TfO in BMIm/TfO)	N	25–50	0.21 (30°C)	400	Sodium-ion battery	[147]
(PVdF-HFP)–(0.5M Na/TfO in EMIm/TfO)	N	25–50	0.25 (30°C)	400	″	[147]
(PVdF-HFP)–(1M Na/TFSI in BMIm/TFSI) (20-70%)	N	30–100	1.9 (30°C)	368–394	″	[148]
(PVdF-HFP)–[1M Na/TFSI in (EC-DEC/TEGDME/EMIm/BF_4)] (75%)	N	30–70	4.7 (70°C)		″	[149]
(PVdF-HFP)–Na/NCS (30%)–EMIm/TCM (0–10%)	N	RT	0.78		Electrochemical double layer capacitor	[150]
[(PVdF-HFP)+rGO-PEG-NH_2 (0–5%)]–EMIm/TFSI (30–50%)–Li/TFSI (20%)	AH	30–100	2.1 (30°C)	315–342	Lithium-ion battery	[151]
(PVdF-HFP)–EMIm/TFSI(0–50%)–(1M Li/TFSI in DME/DOL(1:1))(40–60%)	N	25–75	0.88 (RT)	400	Rechargeable lithium-ion battery	[152]
(PVdF-HFP)–EMIm/TFSI (33%)–Li/TFSI (23.5%)–SiO_2 (20%)	N	25–100	0.74 (25 °C)	300	Lithium-ion battery	[153]
[(PVdF-HFP)–Li/TFSI (20%)]–EMIm/TFSI (80%)	AH	30–50	0.64 (30°C)	200	″	[154]
[(PVdF-HFP)–Li/TFSI (20%)]–BMIm/BF_4 (0–60%)	0.5 ppm	RT	1.7	300–400	Rechargeable lithium-ion battery	[155]
[(PVdF-HFP)–Li/TFSI (20%)]–BMIm/BF_4 (0–70%)	0.5 ppm	RT	3.2	300–400	Lithium-metal battery	[156]
(PVdF-HFP)–(0.5M Li/TFSA in EMIm/TFSA) (90%)	0.5 ppm	10–50	1.7 (20°C)		Lithium-ion battery	[157]
(PVdF-HFP)–EMIm/TFSI (20–60%)–Li/TFSI (20%)	AH	25	4.3		″	[158]
[(PVdF-HFP)–Li/TFSI(20%)]–BMIm/TFSI(0–70%)	AH	30–160	2.07 (30°C)	300–350	″	[133]
(PVdF-HFP)–Li/TFSI (25.33%)–EMIm/TFSI (33–50%)	N	20–80	4.6 (30 °C)		″	[159]
(PVdF-HFP)–BMIm/TFSI (60%)–Li/TFSI (20%)	AH	30–90	1.8 (30°C)		″	[160]
[(PVdF-HFP)+SiO_2(2%)]–BMIm/TFSI(60%)–Li/TFSI(20%)	AH	30–90	5.23 (30°C)		″	[160]
[(PVdF-HFP)+SiO_2(2.8%)]–EMIm/TFSI(55.6%)–Li/TFSI(13.9%)	AH	20–60	1.53 (20°C)		Supercapacitor	[161]

Table 2. (Contd.)

Membrane	*RH*, %	*T*, °C	κ, mS/cm	T_{dec}, °C	Application	Reference
[(PVdF-HFP)+Poly(VPIM/TFSI)]–EMIm/TFSI–Li/TFSI	N	25–85	0.92 (RT)	352	Lithium-ion battery	[162]
[(PVdF-HFP)+SiO_2 + Poly(VPIM/TFSI)]–EMIm/TFSI–Li/TFSI	N	25–85	1.69 (RT)	368	″	[162]
[(PVdF-HFP)+Poly(VPIM/TFSI)]–BMIm/TFSI–Li/TFSI	N	25–85	0.7 (RT)	362	″	[163]
[(PVdF-HFP)+TiO_2]–(0.1–0.5M Li/TFSI в C_3CNMIm/TFSI)	AH	20–70	0.3 (20°C)	200	″	[164]
[(PVdF-HFP)+Al_2O_2 (1.5-1.8%)]–BMIm/BF_4 (11-27%)–Li/TFSI (12–14.5%)–(PC+EC)(1 : 1) (30–36%)	N	25–75	5.26 (25°C)	150	″	[165]
(PVdF-HFP)–PDEIm/TFSI (60%)–(1M Li/TFSI in EC/DMC(1 : 1))	N	25–80	1.78 (25°C)	350	″	[166]
[(PVdF-HFP)+SiO_2 (30%)]–[1M Li/TFSI in [EMIm/TFSI (25–100%)+EC/DEC]	0.1	25–100	4.0 (RT)*	145–198	Lithium-metal battery	[167]
[(PVdF-HFP)–EMIm/TFSI (75%)]–[1M Li/PF_6 in EC:DEC(1 : 1)]	N	25	14.8		Supercapacitor	[125]
[(PVdF-HFP)–LASGP (9%)–EMIm/TFSI (75%)]–[1M Li/PF_6 in EC:DEC(1 : 1)]	N	25	78		″	[125]
[(PVdF-HFP)–Li/BF_4 (15%)]–BMIm/BF_4 (5–20%)	N	30–90	0.02 (RT)		Lithium-ion battery	[168]
(PVdF-HFP)–(0.3M Li/BF_4 in BMIm/BF_4) (20–80%)	AH	30–160	5 (30°C)*	300–380	Electrochemical device	[169]
[(PVdF-HFP)+SiO_2]–(0.3M Li/TfO in EMIm/TfO)(50-65%)	AH	−30–80	3 (30°C)	320–330	Lithium-ion battery	[170]
(PVdF-HFP)–(0.3M Li/TfO in EMIm/TfO) (80%)	N	25–85	4.5 (RT)		Supercapacitor	[171]
(PVdF-HFP)–(0.3M Li/TfO in EMIm/TfO) (65%)–EC/PC(1 : 1) (15%)	N	25–85	8 (RT)		″	[171]
(PVdF-HFP)–(1M Li/NfO in EMIm/NfO) (60–80%)	AH	−50–100	3.09 (30°C)	330	Lithium-ion battery	[172]
(PVdF-HFP)–(1M Li/NfO in BMIm/NfO) (60–80%)	AH	−50–100	26.1 (100°C)	336	Rechargeable lithium-ion battery	[173]
(PVdF-HFP)–EMIm/DCA (60%)–$LiClO_4$ (10%)	N	RT	0.6	300	Lithium-ion battery	[174]

RT: room temperature, AH: anhydrous conditions, FH: full hydration.
[a] Number of moles of ionic liquid–acid per 1 mol of the repeat unit of PBI.
[b] Number of moles of ionic liquid per 1 g of the polymer/copolymer.
N: not stated.
* The value taken from the plot.
**Absorption, %.

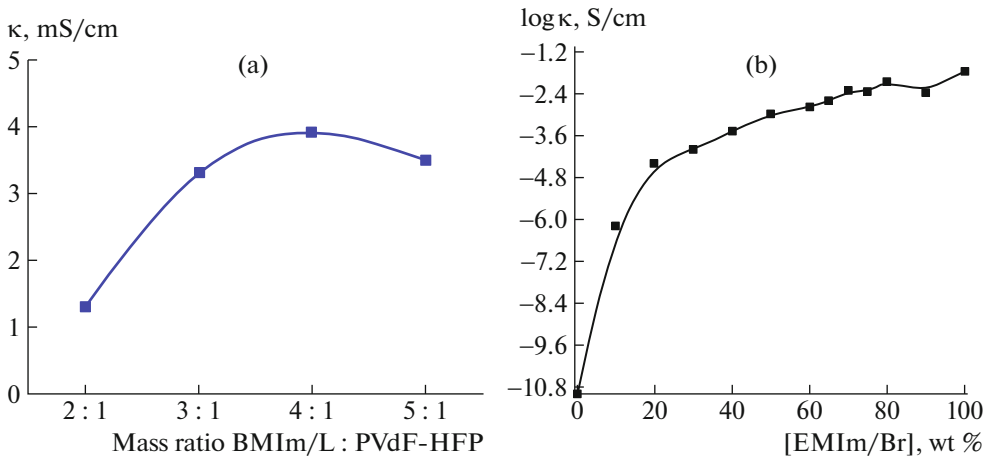

Fig. 7. Room-temperature electroconductivity of the (PVdF–HFP)–ionic liquid as function of the ionic liquid concentration: BMIm/I (a) [134], EMIm/Br (b) [140].

of the ionic liquid (at 450 wt %) the polymer became very fragile and could be hardly processed. Electrochemical window of the film with the composition optimized in view of the electroconductivity and mechanical strength was of 2 V.

The effect of ether substituent in the imidazolium- and ammonium-based ionic liquids on the parameters of electrochemical double layer capacitors (EDLC) consisting of gel polymer electrolyte (PVdF–HFP)–ionic liquid and electrode of reduced graphene oxide was investigated in [141]. Although the size of ammonium cations and viscosity of their ionic liquid was higher in comparison with the salts containing imidazolium cations, electroconductivity was higher in the former case. According to the authors, there were two reasons for that behavior, both reducing the physical interaction between the polymer matrix and the ionic liquid: 1) hydrophobic nature of PVdF–HFP possibly allowed immobilization of cation ether groups exhibiting relatively higher hydrophilicity and 2) three-dimensional structure of the ammonium cations suppressed the stacking which could occur in the π-system due to relatively planar structure of the imidazolium cations. Moreover, the ionic liquids containing the ammonium cations stronger reduced the crystallinity degree of PVdF–HFP in comparison with the imidazolium-containing ionic liquids. The obtained results showed that the presence of ether groups in the imidazolium-based ionic liquids and of longer ester groups in the ammonium-based ionic liquid could enhance the capacity due to denser packing of the ions at the electrode interface.

The influence of the alkylammonium cations on thermal (temperatures of phase transitions and decomposition) and electrochemical (electroconductivity and electrochemical window) parameters of the PVdF–HFP membranes doped with protic ionic liquids based on trifluoroacetate anion and diethyl-, dimethylethyl-, triethyl-, tributyl-, diisopropylethyl-, or triethanolammonium was investigated in [142]. Electroconductivity of the prepared membranes was increased along the TBA(DIPEA)–TEA(TEOA)–DMEA(DEA) series of cations. The membranes exhibited wide electrochemical window, of 6.1–7.6 V at 50°C, narrowing with the increase in temperature. The highest value of electrochemical window was observed for the membrane with TBA/TFA, whereas the lowest value was revealed by the membrane with DMEA/TFA.

Carbon nanotubes (CNTs) were introduced in the (PVdF–HFP)–BMIm/I polymer electrolyte to increase its ionic conductivity [134]. The ionic conductivity passed through a maximum with the increase in the CNTs/PVdF–HFP mass ratio (Fig. 8a). At the CNTs/PVdF–HFP mass ratio of 2 : 1000, the highest ionic conductivity 17.6 mS/cm was reached, which was almost 4.5 times higher in comparison with the (PVdF–HFP)–BMIm/I polymer electrolyte without CNTs. The increase in ionic conductivity with addition of CNTs was likely due to the formation of network of channels in the polymer electrolyte, accelerating the ions transport, and favored dissociation of the ionic liquid which increased the ions concentration. However, addition of too much of CNTs can block the ions transfer, which reduced the ionic conductivity.

Similar effect of addition of graphene oxide (GO) on electroconductivity of the (PVdF–HFP)–EMIm/BF_4 polymer electrolyte was investigated in [126]. The introduction of small amount of graphene oxide (1 wt %) in the polymer electrolyte led to sharp increase in the ionic conductivity (by ~ 260% in comparison with pure polymer electrolyte). Owing to numerous oxygen-containing functional groups at the surface and edges of the sheets, graphene oxide interacted with the copolymer to form the amorphous phase and thus to increase ionic conductivity of the

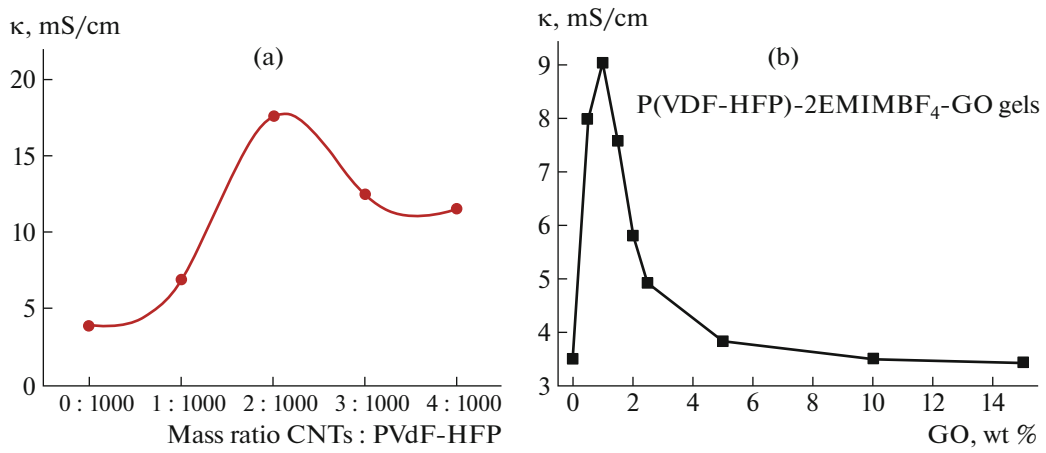

Fig. 8. Electroconductivity of the (PVdF-HFP)–BMIm/I–CNTs polymer electrolytes with different CNTs : PVdF–HFP ratios at the BMIm/I : PVdF–HFP mass ratio 4 : 1 [134] (a); electroconductivity of the (PVdF–HFP)–EMIm/BF_4–graphene oxide (GO) polymer electrolyte as function of the graphene oxide content (b). Mass ratio EMIm/BF_4 : PVdF–HFP is 2 [126].

polymer electrolyte. Moreover, uniform distribution of graphene oxide as three-dimensional network in (PVdF–HFP)–EMIm/BF_4 led to the formation of network of continuous interconnected channels facilitating the ion transfer, which also led to significant increase in the ionic conductivity. With further increase in the content of graphene oxide in the polymer electrolyte, its excess amount blocked those transport channels, which reduced the electroconductivity (Fig. 8b). The solid-state supercapacitor produced with the (PVdF–HFP)–2EMIm/BF_4–graphene oxide polymer electrolyte exhibited lower internal resistance, higher capacity, and better cycling stability as compared to the supercapacitors with (PVdF–HFP)–2EMIm/BF_4 and EMIm/BF_4. The observed excellent parameters were due to high ionic conductivity, perfect compatibility with carbon electrodes, and prolonged stability of the polymer electrolyte doped with graphene oxide.

The increase in concentration of multilayer graphene nanosheets (ad-GNSs) used as the filler led initially to almost twofold increase in electroconductivity of the (PVdF–HFP)–EMIm/TFSI polymer electrolyte, followed by its insignificant decrease with further increase in the ad-GNSs concentration [128]. The obtained (PVdF–HFP)–EMIm/TFSI–(ad-GNSs) polymer electrolyte exhibited very good thermal stability (up to 400°C) and wide electrochemical window (3 V). The solid-state supercapacitor based on commercial active carbon and the modified polymer electrolyte showed the electrochemical parameters improved in comparison with the corresponding all-solid supercapacitor assembled using the (PVdF–HFP)–EMIm/TFSI polymer electrolyte without ad-GNSs additive. In particular, lower internal resistance and charge transfer resistance, higher specific capacity, and better rate and cycling stability parameters were observed.

The investigation of the effect of inorganic fillers, TiO_2 and ZnO nanoparticles, on the properties of the (PVdF–HFP)–EMIm/BF_4 polymer electrolyte [119] revealed that the nanoparticles, similarly to the ionic liquid, decreased the crystallinity degree of PVdF–HFP upon their incorporation in the polymer matrix. However, significant increase in the electroconductivity was not observed. The EDLC cell assembled using the polymer electrolyte with addition of TiO_2 exhibited higher capacity in comparison with the ZnO nanoparticles, due to higher dielectric constant of TiO_2, which favored the ionic liquid dissociation. At the first cycle, specific energy density and specific power of the EDLC cell assembled using the TiO_2-filled electrolyte were 33.19 W h/kg and 1.17 kW/kg, respectively, at specific current of 1 A/g.

In contrast to the above-discussed study [119], the introduction of the $Li_{1.5}Al_{0.33}Sc_{0.17}Ge_{1.5}(PO_4)_3$ (LASGP) ceramic filler into the (PVdF-HFP)–EMIm/TFSI polymer electrolyte led to significant increase in the electroconductivity [125], and also improved mechanical strength as well as electrochemical stability of the films.

Composite polymer electrolyte based on PVdF–HFP, ionic liquid EMIm/BF_4, and organic filler succinonitrile was prepared in [122]. Partial substitution of the ionic liquid in the (PVdF–HFP)–BMIm/BF_4 polymer electrolyte with succinonitrile led to the electroconductivity increase. The presence of nonionic highly polar succinonitrile, exhibiting fast molecular diffusion, waxy nature, good solvating ability, and high dielectric constant, reduced the PVdF–HFP crystallinity, favored the ionic liquid dissociation, and increased the ions mobility. The polymer electrolyte

containing optimized ionic liquid : succinonitrile ratio exhibited ionic conductivity 6.40 mS/cm at room temperature and electrochemical stability range of 2.9–2.5 V. The symmetrical carbon-carbon all-solid supercapacitor cell with that polymer electrolyte showed specific capacity 176 F/g at 0.18 A/g and 138 F/g at 8 A/g, the maximum power being 24.5 kW/kg and energy density being 36 W h/kg at specific current 1.5 A/g.

Hence, the properties making the (PVdF–HFP)–ionic liquid systems promising polymer electrolytes for application in various electrochemical devices are mainly their sufficiently high room-temperature ionic conductivity (10^{-2} S/cm), high electrochemical stability (up to 5 V), and broad operating temperature range (up to 300–400°C).

(PVdF–HFP)–Ionic Liquid–Li/Na Salt Polymer Electrolyte

Polymer electrolytes for lithium power sources with PVdF–HFP as the polymer matrix have been considered in numerous studies. In such polymer electrolytes, ionic liquids act as lithium salt solvent or as plasticizer, when lithium salt in organic solvent is used.

Electrochemical parameters of polymer electrolytes prepared via impregnation of porous PVdF–HFP with sodium salts solutions in ionic liquids (EMIm/TFSI and BMIm/TFSI) and in organic solvents (propylene carbonate and fluoroethylene carbonate) were compared in [147]. The electrolyte based on the ionic liquids revealed such advantages as high thermal stability, nonvolatility, and wide electrochemical window, but its high viscosity hindered the sodium ions mobility in the liquid as well as in the polymer matrix. Moreover, sodium ions in the polymer electrolytes based on ionic liquids was involved in strong interactions with other ions, which also reduced their mobility. Electroconductivity of such polymer electrolyte was five times lower (about 0.21 and 0.25 mS/cm at 30°C) in comparison with the polymer electrolyte based on the sodium salts in the organic solvents. The values of room-temperature electroconductivity of the PVdF–HFP-based polymer electrolytes doped with solutions of LiTFSI in 1-butyl-3-methylimidazolium tetrafluoroborate (BMIm/BF_4) [155, 156, 165], in 1-ethyl-3-methylimidazolium bis(trifluoromethylsulfonyl)imide (EMIm/TFSI) [151–153, 157–159, 161, 162, 167], and in 1-butyl-3-methylimidazolium bis(trifluoromethylsulfonyl)imide (BMIm/TFSI) [133, 160, 163] were in the 1–5 mS/cm range, depending on the doping method. Similarly to the above-discussed influence of the ionic liquid concentration on electroconductivity of the (PVdF–HFP)–ionic liquid polymer electrolyte, electroconductivity of the (PVdF–HFP)–ionic liquid–lithium salt electrolyte passed through maximum with the increase in the ionic liquid content [152, 167]. As was shown in [151, 160, 164, 170], introduction of fillers in the polymer matrix also increased the electroconductivity, but the effect was less prominent, and electroconductivities of the filled and unfilled electrolytes were of the same order. At the same time, it should be noted that the introduction of the fillers enhanced thermal and electrochemical stability of the polymer electrolytes. More significant increase in the electroconductivity (by 1–2 orders of magnitude) was observed in the systems with ionic liquids as plasticizer, the polymer matrix doping being performed by lithium salt solution in an organic solvent [125].

Similar results were obtained in [148] for the polymer electrolyte with the sodium salt (NaTFSI) solution in the ionic liquid (BMIm/TFSI) was introduced in the PVdF–HFP polymer matrix. The ionic conductivity was increased with the increase in the solution content in the polymer electrolyte, the highest value (1.9×10^{-3} S/cm at 30°C being reached at the solution content of 70%; the polymer electrolyte was thermally stable up to 368°C and exhibited wide electrochemical window of 4.2 V. Formation of the polar β-phase in the matrix was observed in the presence of the solution, and its fraction was increased with the growing content of the solution. Furthermore, the vitrification temperature was decreased with the increase in the solution content, due to its plasticizing effect. Electrochemical efficiency of the half-cell (Na-NMC/PE/Na) was studied, with PE being the polymer electrolyte of the optimized composition acting as separator, Na-NMC cathode, and Na metal anode. The cell exhibited specific discharge capacity 108 mA h g^{-1} at discharge rate 0.1°C. The capacity retention (94% upon 200 charge-discharge cycles) was also high.

Comparative analysis of the data on polymer electrolytes with poly(ethylene oxide), PVdF, PVdF-HFP, poly(methyl methacrylate), polyacrylonitrile, poly(vinyl chloride), and polyacrylates as the matrix revealed [176] that PVdF–HFP was the most promising polymer for the development of novel electrolytes for lithium power sources.

CONCLUSION

Polymer electrolytes based on ionic liquids provide an excellent alternative to liquid electrolytes and can be applied in various electrochemical devices, owing to good ionic conductivity as well as mechanical, thermal, chemical, and electrochemical stability. Herein we reviewed the literature on the polymer electrolytes of the polymer + ionic liquid type as well as composite systems based on them, used as membranes in fuel cells, batteries, and supercapacitors. Polybenzimidazole and poly(vinylidene fluoride-*co*-hexafluoropropylene) were considered as polymer matrices, and major

attention was paid to ionic liquids containing alkylammonium and alkylimidazolium cations.

Polybenzimidazoles doped with proton-generating additives are currently the most promising materials for the production of proton-conducting membranes to be used in intermediate-temperature fuel cells. Using protic ionic liquids as proton conductors for the PBI membrane has allowed significant extension of the operating temperature range of the fuel cells towards high temperature in comparison with the PBI–acid membranes. Introduction of a ionic liquid in the PBI–acid polymer membrane improves mechanical properties of the membrane as well as its thermal stability and electroconductivity.

The use of PVdF–HFP as the matrix for the production of polymer electrolytes has led to the increase in solubility in different organic solvents, decrease in the crystallinity, and enhancement of the mechanical strength. The (PVdF–HFP)–ionic liquid polymer electrolytes have exhibited sufficiently high room-temperature ionic conductivity, good electrochemical stability, and wide range of the operation temperature.

Numerous studies have revealed that ionic liquids in the (PVdF–HFP)–ionic liquid–Li/Na salt polymer electrolytes provide promising alternatives to conventional organic plasticizers (ethylene carbonate, propylene carbonate, diethyl carbonate, poly(ethylene glycol), etc.) in view of the chemical power sources applications, owing to their unique properties (high ionic conductivity, wide electrochemical window, inflammability, low vapor pressure, excellent miscibility with conventional liquid electrolytes, and good thermal stability).

It has been shown that introduction of inorganic fillers (silicon dioxide, titanium dioxide, zirconium dioxide, graphene oxide, carbon nanotubes, or layered silicates) in the considered polymer electrolytes improves their mechanical, thermal, and chemical properties.

APPENDIX

ABBREVIATIONS

Cations

AEIm	3-Allyl-1-ethylimidazolium
AMIm	3-Allyl-1-methylimidazolium
AMEtA	*N*-Methyl-2-(2-methoxyethoxy)-*N*,*N*-bis[2-(2-methoxyethoxy)ethyl]ethane-1-ammonium
AMEtIm	*N*-Methyl-2-(2-methoxyethoxy)-*N*,*N*-bis[2-(2-methoxyethoxy)ethyl]imidazolium
ApMIm	1-(3-Aminopropyl)-3-methylimidazolium
BIm	1-Butylimidazolium
BMIm	1-Butyl-3-methylimidazolium
C_3CNMIm	1-Cyanomethyl-3-methylimidazolium
DEA	Diethylammonium
DEMA	Diethylmethylammonium
DEMMsA	*N*,*N*-Diethyl-*N*-methyl-*N*-(2-methoxyethyl)ammonium
DIPEA	Diisopropylethylammonium
DMEA	Dimethylethylammonium
DMEtOHA	*N*,*N*-Dimethyl-*N*-(2-hydroxyethyl)ammonium
EIm	1-H-3-Ethylimidazolium
EMIm	1-Ethyl-3-methylimidazolium
HMIm	1-Hexyl-3-methylimidazolium
MIm	1-H-3-Methylimidazolium
MMEtA	*N*-Methyl-*N*-tris(2-methoxyethyl)ammonium
MsMIm	1-(3-Trimethoxysilylpropyl)-3-methylimidazolium
MtOHTMA	(2-Hydroxymethyl)trimethylammonium
OHEMIm	1-(2-Hydroxyethyl)-3-methylimidazolium
PDEIm	Poly(1,2-diethoxyethylimidazolium)
Pr(MIm)$_2$	1,3-Di(3-methylimidazolium)propane
SEMA	2-Sulfoethylmethylammonum
TBA	Tributylammonium

TEA	Triethylammonium
TEOA	Triethanolammonium
TESPA	Triethyl(3-sulfopropyl)ammonium
TetEA	Tetraethylammonium

Polymers

PBI	Poly-2,2'-(*m*-phenylene)-5,5'-di(benzimidazole)
PBI-O-Ph	Derivative of polybenzimidazole bearing benzofuran fragments
P(MMA-*co*-BMA)	Poly(methyl methacrylate–*co*–butyl methacrylate)
pPBI	Porous polybenzimidazole
PVdF-HFP	Poly(vinylidene fluoride-*co*-hexafluoropropylene)
PVP	Poly(*N*-vinylpyrrolidone)
SPEEK	Sulfonated poly(ether ether ketone)

Anions

BF_4	Tetrafluoroborate
Br	Bromide
CF_3BF_3	Trifluoro(trifluoromethyl)borate
$C_2F_5BF_3$	(Perfluoroethyl)trifluoroborate
$(CH_3)_2PO_4$	Dimethylphosphate
Cl	Chloride
DCA	Dicyanamide
H_2PO_4	Dihydrophosphate
HSO_4	Hydrosulfate
I	Iodide
NCS	Thiocyanate
NfO	Nonafluoro-1-butanesulfonate
PF_6	Hexafluorophosphate
TCB	Tetracyanoborate
TCM	Tricyanomethanide
TFA	Trifluoroacetate
TfO	Trifluoromethanesulfonate
TFSI	Bis(trifluoromethylsulfonyl)imide

Fillers

CNTs	Carbon nanotubes
ETS	Functionalized microporous titanosilicate-type material
GNSs	Graphene nanosheets
GO	Graphene oxide
rGO-PEG-NH_2	2,2''-(Ethylenedioxy)bis(ethylamine) covalently linked to reduced graphene oxide
IPTS	3-(Triethoxysilyl)propyl isocyanate
LASGP	$Li_{1.5}Al_{0.33}Sc_{0.17}Ge_{1.5}(PO_4)_3$
MDA	Melamine-based dendrimer functionalized with mesoporous silica SBA-15
NaY	Sodium-type zeolite
NH_4BEA	Large-pores zeolite
SiO_2–poly(VPIM/TFSI)	Ionic liquid covalently bound to silica nanoparticles
SN	Succinonitrile
SWCNT	Single-wall Carbon Nanotubes
TAIC	Triallylisocyanurate

Solvents

DEC	Diethyl carbonate
DMC	Dimethyl carbonate
DME	Dimethoxyethane
DMF	Dimethylformamide
DOL	Dioxolane
EC	Ethylene carbonate
PC	Propylene carbonate
TEGDME	Tetra(ethylene glycol) dimethyl ether

CONFLICT OF INTERESTS

The authors declare that they have no conflicts of interest.

REFERENCES

1. N. Terasawa and K. Asaka, Mater. Today: Proc. **20**, 265 (2020).
2. A. K. Natha and R. Talukdar, Int. J. Polym. Anal. Charact. **25** (8), 597 (2020).
3. J. Lan, Y. Li, B. Yan, C. Yin, R. Ran, and L.-Y. Shi, ACS Appl. Mater. Interfaces **12**, 37597 (2020).
4. Z. Ullah, A. S. Khan, N. Muhammad, R. Ullah, A. S. Alqahtani, S. N. Sha, O. B. Ghanem, M. A. Bustam, and Z. Man, J. Mol. Liq. **266**, 673 (2018).
5. S. Singhal, S. Agarwal, M. Singh, S. Rana, S. Arora, and N. Singhal, J. Mol. Liq. **285**, 299 (2019).
6. E. A. Chernikova, L. M. Glukhov, V. G. Krasovskiy, L. M. Kustov, M. G. Vorobyeva, and A. A. Koroteev, Russ. Chem. Rev. **84** (8), 875 (2015).
7. E. Fabre and S. M. S. Murshed, J. Mater. Chem. A **9**, 15861 (2021).
8. A. Alashkar, A. Al-Othman, M. Tawalbeh, and M. Qasim, Membranes **12** (2), 178 (2022).
9. C. Liu, B. Chen, W. Shi, W. Huang, and H. Qian, Mol. Pharmaceutics **19** (4), 1033 (2022).
10. L. Sun, K. Zhuo, Y. Chen, Q. Du, S. Zhang, and J. Wang, Adv. Funct. Mater. **32** (27), 2203611 (2022).
11. W. Zhuang, K. Hachem, D. Bokov, M. J. Ansari, and A. T. Nakhjiri, J. Mol. Liq. **349**, 118145 (2022).
12. G. Kaur, H. Kumar, and M. Singla, J. Mol. Liq. **351**, 118556 (2022).
13. W. Jiang, X. Li, G. Gao, F. Wu, C. Luo, and L. Zhang, Chem. Eng. J. **445**, 136767 (2022).
14. P. A. Yudaev and E. M. Chistyakov, Chem. Eng. Sci. **6** (1), 6 (2022).
15. S. K. Singh and A. W. Savoy, J. Mol. Liq. **297**, 112038 (2020).
16. O. Lebedeva, D. Kultin, and L. Kustov, Nanomaterials **11** (12), 3270 (2021).
17. T. M. Dhameliya, P. R. Nagar, K. A. Bhakhar, H. R. Jivani, B. J. Shah, K. M. Patel, V. S. Patel, A. H. Soni, L. P. Joshi, and N. D. Gajjar, J. Mol. Liq. **348**, 118329 (2022).
18. B. Karimi, M. Tavakolian, M. Akbari, and F. Mansouri, ChemCatChem **10** (15), 3173 (2018).
19. J. Richter and M. Ruck, Molecules **25** (1), 78 (2020).
20. N. Noroozi-Shad, M. Gholizadeh, and H. Sabet-Sarvestani, J. Mol. Struct. **1257**, 132628 (2022).
21. D. O. Ponkratov, A. S. Shaplov, and Y. S. Vygodskii, Polym. Sci., Ser. C **61** (1), 2 (2019).
22. M. R. Asrami, N. N. Tran, K. D. P. Nigam, and V. Hessel, Sep. Purif. Technol. **262**, 118289 (2021).
23. W.-W. Yan, X.-Y. Wei, M.-X. Wang, and Z.-M. Zong, Ind. Eng. Chem. Res. **61** (13), 4481 (2022).
24. E. Quijada-Maldonado and J. Romero, Curr. Opin. Green Sustainable Chem. **27**, 100428 (2021).
25. B. Kazmi, S. A. A. Taqvi, and S. I. Ali, ChemBioEng Rev. **9** (2), 190 (2022).
26. J. Guo, Z. D. Tucker, Y. Wang, B. L. Ashfeld, and T. Luo, Nat. Commun. **12**, 437 (2021).
27. C. Xu, G. Yang, D. Wu, M. Yao, C. Xing, J. Zhang, H. Zhang, F. Li, Y. Feng, S. Qi, M. Zhuo, and J. Ma, Chem. Asian. J. **16**, 549 (2021).
28. I. Osada, H. de Vries, B. Scrosati, and S. Passerini, Angew. Chem. Int. Ed. **55**, 500 (2016).
29. S. Sultana, K. Ahmed, P. K. Jiwanti, B. Y. Wardhana, and N. I. Shiblee, Gels **8** (1), 2 (2022).
30. H. A. Elwan, R. Thimmappa, M. Mamlouk, and K. Scott, J. Power Sources **510**, 230371 (2021).
31. L. Yin, S. Li, X. Liu, and T. Yan, Sci. China Mater. **62** (11), 1537 (2019).
32. G. G. Eshetu, D. Mecerreyes, M. Forsyth, H. Zhang, and M. Armand, Mol. Syst. Des. Eng. **4**, 294 (2019).
33. A. Ray and B. Saruhan, Materials **14**, 2942 (2021).
34. A. S. Shaplov, D. O. Ponkratov, P. S. Vlasov, E. I. Lozinskaya, I. A. Malyshkina, F. Vidal, P.-H. Aubert, M. Armand, and Y. S. Vygodskii, Polym. Sci., Ser. B **56** (2), 164 (2014).
35. K. S. Egorova and V. P. Ananikov, J. Mol. Liq. **272**, 271 (2018).
36. T. B. V. Dinis, F. A. e Silva, F. Sousa, and M. G. Freire, Materials **14** (21), 6231 (2021).
37. N. Gandhewar and P. Shende, Ionics **27**, 3715 (2021).
38. A. M. Curreri, S. Mitragotri, and E. E. L. Tanner, Adv. Sci. **8**, 2004819 (2021).
39. R. Hayes, G. G. Warr, and R. Atkin, Chem. Rev. **115**, 6357 (2015).
40. P. A. Hunt, C. R. Ashworth, and R. P. Matthews, Chem. Soc. Rev. **44**, 1257 (2015).
41. H. Abe, J. Mol. Liq. **332**, 115189 (2021).

42. O. Nordness and J. F. Brennecke, Chem. Rev. **120**, 12873 (2020).
43. L. E. Shmukler, I. V. Fedorova, Yu. A. Fadeeva, and L. P. Safonova, J. Mol. Liq. **321**, 114350 (2021).
44. E. Fabre and S. M. S. Murshed, J. Mater. Chem. A **9**, 15861 (2021).
45. C. S. Buettner, A. Cognigni, C. Schröder, and K. Bica-Schröder, J. Mol. Liq. **347**, 118160 (2022).
46. A. S. Shaplov, D. O. Ponkratov, and Y. S. Vygodskii, Polym. Sci., Ser. B **58** (2), 73 (2016).
47. A. Kazakov, J. W. Magee, R. D. Chirico, E. Paulechka, V. Diky, C. D. Muzny, K. Kroenlein, and M. Frenkel, "NIST Standard Reference Database 147: NIST Ionic Liquids Database - (ILThermo)," Version 2.0, National Institute of Standards and Technology, Gaithersburg MD, 20899. https://ilthermo.boulder.nist.gov. Accessed August 21, 2023.
48. S. Zhang, X. Lu, Q. Zhou, X. Li, X. Zhang, and S. Li, *Ionic Liquids: Physicochemical Properties* (Elsevier, 2009).
49. V. Bocharova and A. P. Sokolov, Macromolecules **53** (11), 4141 (2020).
50. K. Yue, C. Zhai, S. Gu, J. Yeo, and G. Zhou, Electrochim. Acta **401**, 139527 (2022).
51. J. Atik, J. H. Thienenkamp, G. Brunklaus, M. Winter, and E. Paillard, Electrochim. Acta **398**, 139333 (2021).
52. Y. Yang, Q. Wu, D. Wang, C. Ma, Z. Chen, Q. Su, C. Zhu, and C. Li, J. Membr. Sci. **612**, 118424 (2020).
53. M. T. Musa, N. Shaari, and S. K. Kamarudin, Int. J. Energy Res. **45**, 1309 (2021).
54. K. G. Khatmullina, G. R. Baimuratova, V. A. Lesnichaya, N. I. Shuvalova, and O. V. Yarmolenko, Polym. Sci., Ser. A **60** (2), 222 (2018).
55. S. Ahmad, T. Nawaz, A. Ali, M. F. Orhan, A. Samreen, and A. M. Kannan, Int. J. Hydrogen Energy **47**, 19086 (2022).
56. Z. Guo, J. Chen, J. J. Byun, M. Perez-Page, Z. Ji, Z. Zhao, and S. M. Holmes, J. Membr. Sci. **641**, 119868 (2022).
57. J. Kim, K. Kim, T. Ko, J. Han, and J.-C. Lee, Int. J. Hydrogen Energy **46**, 12254 (2021).
58. S. Kumar, V. S. Manikandan, A. K. Palai, S. Mohanty, and S. K. Nayak, Solid State Ionics **332**, 10 (2019).
59. S. Vinoth, G. Kanimozhi, K. Hari Prasad, Kumar Harish, E. S. Srinadhu, and N. Satyanarayana, Polym. Compos. **40**, 1585 (2019).
60. R. Jamil and D. S. Silvester, Curr. Opin. Electrochem. **35**, 101046 (2022).
61. Shalu, R. K. Singh, and R. Dhar, Int. J. Energy Res. **45**, 15646 (2021).
62. M. Ebrahimi, W. Kujawski, K. Fatyeyeva, and J. Kujawa, Int. J. Mol. Sci. **22**, 5430 (2021).
63. N. Shaari, N. N. R. Ahmad, R. Bahru, and C. P. Leo, Int. J. Energy Res. **46**, 2166 (2022).
64. R. M. L. L. Rathnayake, K. S. Perera, and K. P. Vidanapathirana, AIMS Energy **8** (2), 231 (2020).
65. J. P. Sharma and V. Bharti, IOP Conf. Ser.: Mater. Sci. Eng. **961**, 012005 (2020).
66. G. Yang, Y. Song, Q. Wang, L. Zhang, and L. Deng, Mater. Des. **190**, 108563 (2020).
67. K. S. Khoo, W. Y. Chia, K. Wang, C.-K. Chang, H. Y. Leong, M. N. B. Maaris, and P. L. Show, Sci. Total Environ. **793**, 148705 (2021).
68. J. Escorihuela, J. Olvera-Mancilla, L. Alexandrova, L. F. del Castillo, and V. Vicente Compañ, Polymers **12**, 1861 (2020).
69. C. Y. Wong, W. Y. Wong, K. S. Loh, and K. L. Lim, React. Funct. Polym. **171**, 105160 (2022).
70. L. K. Seng, M. S. Masdar, and L. K. Shyuan, Membranes **11**, 728 (2021).
71. H. A. Elwan, M. Mamlouk, and K. Scott, J. Power Sources **484**, 229197 (2021).
72. P. Bakonyi, L. Koók, T. Rózsenberszki, G. Tóth, K. Bélafi-Bakó, and N. Nemestóthy, Membranes **10**, 16 (2020).
73. I. Vázquez-Fernández, M. Raghibi, A. Bouzina, L. Timperman, J. Bigarré, and M. Anouti, J. Energy Chem. **53**, 197 (2021).
74. I. Vázquez-Fernández, A. Bouzina, M. Raghibi, L. Timperman, J. Bigarré, and M. Anouti, J. Mater. Sci. **55**, 16697 (2020).
75. S. Mondal, F. Papiya, S. N. Ash, and P. P. Kundu, J. Environ. Chem. Eng. **9**, 104945 (2021).
76. S. R. Kumar, J.-J. Wang, Y.-S. Wu, C.-C. Yang, and S. J. Lue, J. Power Sources **445**, 227293 (2020).
77. C. Hou, X. Zhang, Y. Li, G. Zhou, and J. Wang, J. Membr. Sci. **550**, 136 (2018).
78. P. Kumar and R. P. Bharti, J. Electrochem. Soc. **166** (15), F1190 (2019).
79. K. Karuppasamy, J. Theerthagiri, D. Vikraman, C.-J. Yim, S. Hussain, R. Sharma, T. Maiyalagan, J. Qin, and H.-S. Kim, Polymers **12**, 918 (2020).
80. E. Josef, Y. Yan, M. C. Stan, J. Wellmann, A. Vizintin, M. Winter, P. Johansson, R. Dominko, and R. Guterman, Isr. J. Chem. **59**, 832 (2019).
81. X. Tang, S. Lv, K. Jiang, G. Zhou, and X. Liu, J. Power Sources **542**, 231792 (2022).
82. M. J. Park, I. Choi, J. Hong, and O. Kim, J. Appl. Polym. Sci. **129**, 2363 (2013).
83. W. Ye, H. Wang, J. Ning, Y. Zhong, and Y. Hu, J. Energy Chem. **57**, 219 (2021).
84. Y.-S. Ye, J. Rick, and B. Hwang, J. Mater. Chem. A **1**, 2719 (2013).
85. J. Lin, S. Willbold, T. Zinkevich, S. Indris, and C. Korte, J. Mol. Liq. **342**, 116964 (2021).
86. B. Niu, S. Luo, C. Lu, W. Yi, J. Liang, S. Guo, D. Wang, F. Zeng, S. Duan, Y. Liu, L. Zhang, and B. Xu, Solid State Ionics **361**, 115569 (2021).
87. S. Liu, L. Zhou, P. Wang, F. Zhang, S. Yu, Z. Shao, and B. Yi, ACS Appl. Mater. Interfaces **6**, 3195 (2014).
88. G. Skorikova, D. Rauber, D. Aili, S. Martin, Q. Li, D. Henkensmeier, and R. Hempelmann, J. Membr. Sci. **608**, 118188 (2020).
89. M. Mamlouk, P. Ocon, and K. Scott, J. Power Sources **245**, 915 (2014).
90. J. Lin and C. Korte, Fuel Cells **20** (4), 461 (2020).
91. Yu. A. Fadeeva, S. M. Kuzmin, L. E. Shmukler, and L. P. Safonova, Russ. Chem. Bull. **70** (1), 56 (2021).

92. V. Compañ, J. Escorihuela, J. Olvera, A. García-Bernabe, and A. Andrio, Electrochim. Acta **354**, 136666 (2020).
93. J. T.-W. Wang and S. L.-C. Hsu, Electrochim. Acta **56**, 2842 (2011).
94. E. Van de Ven, A. Chairuna, G. Merle, S. P. Benito, Z. Borneman, and K. Nijmeijer, J. Power Sources **222**, 202 (2013).
95. A. Eguizabal, J. Lemus, V. Roda, M. Urbiztondo, F. Barreras, and M. P. Pina, Int. J. Hydrog. Energy **37**, 7221 (2012).
96. L. G. Trindade, L. Zanchet, P. C. Martins, K. M. N. Borba, R. D. M. Santos, R. S. Paiva, L. A. F. Vermeersch, E. A. Ticianelli, M. O. Souza, and E. M. A. Martini, Polymer **179**, 121723 (2019).
97. J. Schauer, A. Sikora, M. Plišková, J. Mališ, P. Mazúrb, M. Paidar, and K. Bouzek, J. Membr. Sci. **367**, 332 (2011).
98. Z. Rajabi, M. Javanbakht, K. Hooshyari, A. Badieid, and M. Adibi, New J. Chem. **44**, 5001 (2020).
99. T. Mao, S. Wang, X. Wang, F. Liu, J. Li, H. Chen, D. Wang, G. Liu, J. Xu, and Z. Wang, ACS Appl. Mater. Interfaces **11**, 17742 (2019).
100. J. Escorihuela, A. García-Bernabé, Á. Montero, Ó. Sahuquillo, E. Giménez, and V. Compañ, Polymers **11**, 732 (2019).
101. X. Wang, S. Wang, C. Liu, J. Li, F. Liu, X. Tian, H. Chen, T. Mao, J. Xu, and Z. Wang, Electrochim. Acta **283**, 691 (2018).
102. C. Xu, X. Liu, J. Cheng, and K. Scott, J. Power Sources **274**, 922 (2015).
103. A. Eguizábal, J. Lemus, and M. P. Pina, J. Power Sources **222**, 483 (2013).
104. T. Xiao, R. Wang, Z. Chang, Z. Fang, Z. Zhu, and C. Xu, Prog. Nat. Sci.: Mater. Int. **30**, 743 (2020).
105. D. Aili, D. Henkensmeier, S. Martin, B. Singh, Y. Hu, J. O. Jensen, L. N. Cleemann, and Q. Li, Electrochem. Energy Rev. **3**, 793 (2020).
106. S. S. Araya, F. Zhou, V. Liso, S. L. Sahlin, J. R. Vang, S. Thomas, X. Gao, C. Jeppesen, and S. K. Kœr, Int. J. Hydrogen Energy **41**, 21310 (2016).
107. E. Quartarone and P. Mustarelli, Energy Environ. Sci. **5**, 6436 (2012).
108. J. Li, X. Li, S. Yu, J. Hao, W. Lu, Z. Shao, and B. Yi, Energy Convers. Manage. **85**, 323 (2014).
109. K. A. Perry, K. L. More, E. A. Payzant, R. A. Meisner, B. G. Sumpter, and B. C. Benicewicz, J. Polym. Sci., Part B: Polym. Phys. **52**, 26 (2014).
110. T. K. Maiti, J. Singh, J. Majhi, A. Ahuja, S. Maiti, P. Dixit, S. Bhushan, A. Bandyopadhyay, and S. Chattopadhyay, Polymer **255**, 125151 (2022).
111. E. Qu, X. Hao, M. Xiao, D. Han, S. Huang, Z. Huang, S. Wang, and Y. Meng, J. Power Sources **533**, 231386 (2022).
112. M. A. Haque, A. B. Sulong, K. S. Loh, E. H. Majlan, T. Husaini, and R. E. Rosli, Int. J. Hydrogen Energy **42**, 9156 (2017).
113. S. Subianto, Polym. Int. **63**, 1134 (2014).
114. A. Y. Leikin, E. G. Bulycheva, A. L. Rusanov, and D. Yu. Likhachev, Polym. Sci., Ser. B **48** (5–6), 144 (2006).
115. J. S. Yang, L. N. Cleemann, T. Steenberg, C. Terkelsen, Q. F. Li, J. O. Jensen, H. A. Hjuler, N. J. Bjerrum, and R. H. He, Fuel Cells **14**, 7 (2014).
116. K. Hooshyari, M. Javanbakht, and M. Adibi, Int. J. Hydrogen Energy **42**, 10870 (2016).
117. K. Hooshyari, M. Javanbakht, and M. Adibi, Electrochim. Acta **205**, 142 (2016).
118. Y. A. Dobrovolsky, A. I. Chikin, E. A. Sanginov, and A. V. Chub, ISJAEE **168**, 22 (2015).
119. S. Das and A. Ghosh, J. Appl. Polym. Sci. **137** (22), 48757 (2020).
120. M. Shi, C. Yang, C. Yan, J. Jiang, Y. Liu, Z. Sun, W. Shi, G. Jian, Z. Guo, and J.-H. Ahn, NPG Asia Mater. **11**, 61 (2019).
121. F. Zhou, H. Huang, C. Xiao, S. Zheng, X. Shi, J. Qin, Q. Fu, X. Bao, X. Feng, K. Müllen, and Z.-S. Wu, J. Am. Chem. Soc. **140**, 8198 (2018).
122. G. P. Pandey, T. Liu, C. Hancock, Y. Li, X. S. Sun, and J. Li, J. Power Sources **328**, 510 (2016).
123. A. A. Hor, N. Yadav, and S. A. Hashmi, J. Energy Storage **47**, 103608 (2022).
124. X. Zhang, M. Kar, T. C. Mendes, and Y. Wu, and D. R. MacFarlane, Adv. Energy Mater. **8**, 1702702 (2018).
125. H. G. Redda, Y. Nikodimos, W.-N. Su, R.-S. Chen, S.-K. Jiang, L. H. Abrha, T. M. Hagosb, H. K. Bezabh, H. H. Weldeyohannes, and B. J. Hwang, Mater. Today Commun. **26**, 102102 (2021).
126. X. Yang, F. Zhang, L. Zhang, T. Zhang, Y. Huang, and Y. Chen, Adv. Funct. Mater. **23**, 3353 (2013).
127. J. Guan, Y. Li, and J. Li, Ind. Eng. Chem. Res. **56**, 12456 (2017).
128. M.-J. Shi, S.-Z. Kou, B.-S. Shen, J.-W. Lang, Z. Yang, and X.-B. Yan, Chin. Chem. Lett. **25**, 859 (2014).
129. S. Kumar, P. K. Singh, D. Agarwal, P. S. Dhapola, T. Sharma, S. V. Savilov, E. A. Arkhipova, M. K. Singh, and A. Singh, Phys. Status Solidi A **219** (7), 2100711 (2022).
130. D. Kumar and D. K. Kanchan, J. Energy Storage **22**, 44 (2019).
131. J. Mališ, P. Mazúr, J. Schauer, M. Paidar, and K. Bouzek, Int. J. Hydrogen Energy **38**, 4697 (2013).
132. G. P. Pandey and S. A. Hashmi, J. Mater. Chem. A **1**, 3372 (2013).
133. Shalu, V. K. Singh, and R. K. Singh, J. Mater. Chem. C **3**, 7305 (2015).
134. L.-Q. Fan, Q.-M. Tu, C.-L. Geng, Y.-L. Wang, S.-J. Sun, Y.-F. Huang, and J.-H. Wu, Int. J. Hydrogen Energy **45**, 17131 (2020).
135. J. P. Serra, R. S. Pinto, J. C. Barbosa, D. M. Correia, R. Gonçalves, M. M. Silva, S. Lanceros-Mendez, and C. M. Costa, Sustainable Mater. Technol. **25**, e00176 (2020).
136. M. Tripathi, S. M. Bobade, M. Gupta, and Y. Kumar, Macromol. Symp. **388**, 1900029 (2019).
137. K. Mishra, S. A. Hashmi, and D. K. Rai, J. Solid State Electrochem. **18**, 2255 (2014).
138. M. Tripathi and S. K. Tripathi, Ionics **23**, 2735 (2017).

139. Shalu, S. K. Chaurasia, R. K. Singh, and S. Chandra, J. Phys. Chem. B **117**, 897 (2013).
140. A. Gupta, A. Jain, and S. K. Tripathi, J. Energy Storage **32**, 101723 (2020).
141. S. Siyahjani, S. Oner, H. Diker, B. Gultekin, and C. Varlikli, J. Power Sources **467**, 228353 (2020).
142. L. E. Shmukler, E. V. Glushenkova, Yu. A. Fadeeva, M. S. Gruzdev, N. O. Kudryakova, and L. P. Safonova, J. Mol. Liq. **283**, 338 (2019).
143. N. Terasawa, Diamond Relat. Mater. **95**, 77 (2019).
144. M. G. Nair, S. R. Mohapatra, M.-R. Garda, B. Patanair, A. Saiter-Fourcin, and S. Thomas, Mater. Res. Express **7**, 064005 (2020).
145. M. G. Nair and S. R. Mohapatra, Mater. Lett. **251**, 148 (2019).
146. Harshlata, K. Mishra, and D. K. Rai, Mater. Sci. Eng. B **267**, 115098.
147. D. T. Vo, H. N. Do, T. T. Nguyen, T. T. H. Nguyen, V. M. Tran, S. Okada, and M. L. P. Le, Mater. Sci. Eng. B **241**, 27 (2019).
148. R. Mishra, S. K. Singh, H. Gupta, R. K. Tiwari, D. Meghnani, A. Patel, A. Tiwari, V. K. Tiwari, and R. K. Singh, Energy Fuels **35**, 15153 (2021).
149. M. S. Syali, K. Mishra, D. K. Kanchan, and D. Kumar, J. Mol. Liq. **341**, 116922 (2021).
150. A. T. Manfo, P. K. Singh, R. M. Mehra, R. C. Singh, and M. Gupta, Recent Innovations Chem. Eng. **14**, 21 (2021).
151. P. Xu, H. Chen, X. Zhou, and H. Xiang, J. Membr. Sci. **617**, 118660 (2021).
152. T. Chen, W. Kong, Z. Zhang, L. Wanga, Y. Hu, G. Zhu, R. Chen, L. Ma, W. Yan, Y. Wang, J. Liu, and Z. Jin, Nano Energy **54**, 17 (2018).
153. Q. Guo, Y. Han, H. Wang, S. Xiong, S. Liu, C. Zheng, and K. Xie, Solid State Ionics **321**, 48 (2018).
154. S. K. Singh, H. Gupta, L. Balo, Shalu, V. K. Singh, A. K. Tripathi, Y. L. Verma, and R. K. Singh, Ionics **24**, 1895 (2018).
155. Shalu-Kataria, L. Balo, H. Gupta, V. K. Singh, S. K. Singh, A. K. Tripathi, Y. L. Verma, and R. K. Singh, ECS Trans. **73** (1), 183 (2016).
156. Shalu, L. Balo, H. Gupta, V. K. Singh, and R. K. Singh, RSC Adv. **6**, 73028 (2016).
157. A. Hofmann, M. Schulz, and T. Hanemann, Electrochim. Acta **89**, 823 (2013).
158. J. Bai, H. Lu, Y. Cao, X. Li, and J. Wang, RSC Adv. **7**, 30603 (2017).
159. P. X. Yang, W. Y. Cui, L. B. Li, and L. Liu, and M. Z. An, Solid State Sci. **14**, 598 (2012).
160. S. Kataria, Y. L. Verma, H. Gupta, S. K. Singh, N. Srivastava, R. Dhar, and R. K. Singh, Polym.-Plast. Technol. Mater. **59** (9), 952 (2020).
161. M. Yao, A. Liu, C. Xing, B. Li, S. Pan, J. Zhang, P. Su, and H. Zhang, Chem. Eng. J. **394**, 124883 (2020).
162. T. Huang, M.-C. Long, G. Wu, Y.-Z. Wang, and X.-L. Wang, ChemElectroChem **6**, 3674 (2019).
163. T. Huang, M.-C. Long, X.-L. Wang, G. Wu, and Y.-Z. Wang, Chem. Eng. J. **375**, 122062 (2019).
164. A. Zalewska, J. Dumińska, N. Langwald, J. Syzdek, and M. Zawadzki, Electrochim. Acta **121**, 337 (2014).
165. K. Huang, Y. Wang, H. Mi, D. Ma, B. Yong, and P. Zhang, J. Mater. Chem. A **8**, 20593 (2020).
166. Z. Hu, J. Chen, Y. Guo, J. Zhu, X. Qu, W. Niu, and X. Liu, J. Membr. Sci. **599**, 117827 (2020).
167. Q. Guo, Y. Han, H. Wang, X. Hong, C. Zheng, S. Liu, and K. Xie, RSC Adv. **6**, 101638 (2016).
168. J. Tang, R. Muchakayala, S. Song, M. Wang, and K. N. Kumar, Polym. Test. **50**, 247 (2016).
169. Shalu, S. K. Chaurasia, R. K. Singh, and S. Chandra, J. Appl. Polym. Sci. **132**, 41456 (2015).
170. S. Khurana and A. Chandra, Solid State Ionics **340**, 115027 (2019).
171. Y. Kumar, G. P. Pandey, and S. A. Hashmi, J. Phys. Chem. C **116**, 26118 (2012).
172. K. Karuppasamy, P. Anil Reddy, G. Srinivas, R. Sharma, A. Tewari, G. H. Kumar, and D. Gupta, J. Solid State Electrochem. **21**, 1145 (2017).
173. K. Karuppasamy, P. A. Reddy, G. Srinivas, A. Tewari, R. Sharma, X. S. Shajan, and D. Gupta, J. Membr. Sci. **514**, 350 (2016).
174. Q. Li and H. Ardebili, J. Power Sources **303**, 17 (2016).
175. L. Liu, X. Wang, C. Yang, P. Han, L. Zhang, L. Gao, Z. Wu, B. Liu, and R. Liu, Acta Metall. Sin. (Engl. Lett.) **34**, 417 (2021).
176. Yu. V. Baskakova, O. V. Yarmolenko, and O. N. Efimov, Russ. Chem. Rev. **81** (4), 367 (2012).

Translated by E. Karpushkin